Full Title: Influence of Soil-Pile Foundation-Structure Interaction on the Ductility Capacity of RC Buildings

Short Title: Influence of SPFSI on Ductility Capacity of RC Buildings

Author 1

- Nishant Sharma, Assistant Professor
- Department of Civil Engineering, Institute of Infrastructure Technology Research and Management, Ahmedabad, Gujarat, India

Author 2

- Kaustubh Dasgupta, Associate Professor
- Department of Civil Engineering, Indian Institute of Technology Guwahati, Guwahati, Assam, India
- Adjunct Faculty, Centre for Disaster Management and Research, Indian Institute of Technology Guwahati, Guwahati, Assam, India.

Author 3

- Arindam Dey, Associate Professor
- Department of Civil Engineering, Indian Institute of Technology Guwahati, Guwahati, Assam, India

Full contact details of corresponding authors.

- **Arindam Dey, Department of Civil Engineering, Indian Institute of Technology Guwahati, Guwahati, Assam, India, Pin-781039.**

  Email: arindam.dey@iitg.ac.in

ABSTRACT

A surge in the infrastructure development, in populated regions, has compelled the construction of Reinforced Concrete (RC) buildings to be made over pile foundations when the underlying soil deposit is weak or loose. Individual piles in the foundation system can exhibit significant inelasticity and contribute to the modification in the inelastic response and ductility of the building system. Studies investigating the influence of soil-pile foundation structure interaction (SPFSI) on the inelastic seismic response of RC buildings are scarce. Existing studies on building with pile foundations consider the inelastic behaviour of the soil without accounting for pile inelasticity. Moreover, studies assessing the influence of SPFSI on the ductility of RC buildings are scarcely available. This article investigates the role of the complex phenomenon of SPFSI in modifying the inelastic behaviour and ductility capacity of RC frame and RC wall-frame systems. The results from this study show that the soil-pile foundation system inevitably contributes to the lateral load behaviour of RC buildings through inelastic deformations and rocking of the pile groups. This modifies the inelastic superstructure response in terms of the yield and ultimate drifts which may lead to a decrease in the ductility capacity of the RC buildings. In the present study the decrease in the ductility capacity was observed to be as high as 39% for RC wall-frame system and 12% for RC frame systems. The obtained results imply that, in order to account for the reduction in the ductility capacity of RC buildings under SPFSI effects, the response reduction factor needs to be suitably modified while carrying out the seismic design. Overall, this study reflects the importance of considering the complex phenomenon of soil-pile-foundation structure interaction (SPFSI) and its critical contribution towards the modification in the ductility of RC buildings supported on pile foundations.

KEYWORDS

Soil-pile foundation-structure interaction (SPFSI), RC frame system, RC wall-frame system, ductility, inelastic behavior, finite element analysis

1. INTRODUCTION

The contemporary era has experienced a surge in the construction of Reinforced Concrete (RC) frame buildings especially in the populous areas. In regions of high seismicity these buildings may also possess shear walls for resisting the lateral loads and are termed as RC wall-frame buildings. Depending on the underlying weak soil it may become imperative to adopt piles as the supporting foundational system. Under these conditions, the seismic performance of the structural system can be significantly governed by the mutual interaction of the structure and soil-

pile foundation (SPF) system or in other words soil structure interaction (SSI) effects. Several past and recent studies have affirmed that the dynamic response of structures could be significantly affected by SSI [1-9]. Veletsos and Meek [1] conducted analytical studies on structures idealized as single degree freedom systems and demonstrated that their natural characteristics are modified (i.e., natural period and damping increase) by considering SSI. Similar conclusion was drawn by Wolf [2] through analytical studies and by Luco et al. [3] through full-scaled forced vibration tests. The use of average spectral motion curves without proper normalization of period can thus end in unsafe design [4] of the structure under the influence of SSI. Further, the aspect ratio of the structure (i.e., height to width) along with the flexibility and embedment of the foundation can also significantly influence the response [1, 11-14]. Specifically, SSI effects can lead to an increase in the maximum displacement due to the deformation and rocking [15] at the super structure base [16]. This effect could be significantly greater in the case of sandy soil as for cohesionless soil the effect of soil nonlinearity is greater and could lead to a compromise in the structural safety [6].

Pile foundations are usually considered to exhibit lesser displacements as they possess sufficient restraint against rocking when compared to shallow foundations, and therefore fixed base analysis is conventionally adopted [17]. However, in reality the behaviour of structures on pile foundation cannot be assumed to be the same as that of a fixed base system, especially when the piles can exhibit inelasticity. The deformation at the base of a super-structure can result in significant inelastic rotation and nonlinearity. Especially the piles may exhibit inelasticity at the top regions (pile-pile cap junction) or at the interface of two soil layers with contrasting properties [18] leading to an increase in the interstorey drifts or lateral deflections [13,17,19-20]. Further, rocking of the pile foundations may also contribute to the lateral deflection of the structure [21] and cause a change in the structural performance (e.g., from life safe to collapse) [17,20,22].

Another aspect that determines the seismic performance of RC buildings is the approach using which the building is designed. Past studies have highlighted many instances wherein the force (or strength) based design [23] proved to be inadequate due to the inability of the buildings to undergo large inelastic deformations leading to severe damage or collapse [23]. These observations paved the way for the present-day philosophy of earthquake-resistant design for RC structures [24-25], according to which the deformation capacity is accounted for through the exhibition of ductility. While most past studies on the ductility of RC buildings have ignored SSI effects [26-30], studies on ductility considering SSI effects have focused on buildings supported on shallow foundations [31]. Unlike shallow

foundations (which act as rigid blocks), the pile foundations, owing to its geometry, may exhibit significant inelastic response that in turn may modify the inelastic behavior of the superstructure. This modification in the inelastic behaviour would be instrumental in modifying the ductility of the RC building system under SSI effects. Interestingly, it has been urged in the past to investigate the inelastic response of structures when supported by pile foundation (inelastic foundation) and assess the modification in the overall ductility of the structural system [18]. However, this gap still exists in the literature.

To capture the modifications in the inelastic behaviour and ductility of RC buildings when supported by pile foundation system, it is essential to adopt a suitable approach for its mathematical modelling and analysis. Analytical and numerical procedures are commonly used for investigating the influence of SSI on structural systems. The analytical procedures utilize closed form expressions to obtain the solutions. Although accurate, these solutions employ the simplification of representing buildings as a Single Degree of Freedom (SDOF) oscillator. This approach is not appropriate for modeling non-uniform foundation rocking behavior as found in the case of frame and wall-frame buildings. Further, past investigations based on the analytical approach have mostly been carried out for SDOF systems on circular / rectangular disc resting on (or embedded in) elastic half space [32]. This is because the analytical procedure cannot be applied to the cases where the soil-foundation geometry is complex or wherein nonlinear inelastic behaviour is expected. The numerical procedures, on the other hand, could be utilized for SSI problems with complex geometries and material nonlinearities but can demand substantial effort in modelling and computation [32]. For this reason, not many studies exist that investigate nonlinear soil foundation structure interaction in detail, especially considering pile foundations. The few studies that exist consider single lumped pile foundation [15-22] which may not be a suitable approach to represent piles existing in a group and where non-uniform rocking is exhibited under the various vertical members of the building. Also, these studies are limited to a single type of structural system (frame or wall-frame) and do not consider variation in the soil-pile foundation properties. Further, no study has been carried out that investigates the inelastic behaviour of soil-pile foundation system and its corresponding influence on the ductility capacity of RC buildings.

The objective of the current study is to investigate the complex phenomenon of soil-pile foundation structure interaction (SPFSI) and assess the modification in the (a) inelastic response of the RC buildings, (b) inelastic response of pile foundation system and (c) ductility of RC buildings. To realize the objectives, a numerical study has been

undertaken by considering a broad range of configurations of RC frame and RC wall-frame systems supported by pile foundation embedded in different soil conditions. Detailed finite element modelling has been carried out to capture the complex interaction of the pile group foundation with the vertical members (columns and shear wall) of the RC buildings. Nonlinear pushover analysis has been carried out to study the influence of SSI on the inelastic behavior of the considered systems. Subsequently, the role of foundation rocking and pile inelasticity in modifying the inelastic response of the super-structural system is examined. Finally, the effect of SPFSI on the ductility capacity of RC frame and RC wall-frame systems is outlined.

2. NUMERICAL MODELLING

To incorporate SSI effects, direct modelling approach has been adopted wherein the RC frame and RC wall-frame systems are modelled as a single unit along with the soil-pile foundation system (Figure 1). A finite element software framework, OpenSees [33], has been used to conduct the entire study and the various aspects of the numerical modelling are discussed briefly in the following subsections.

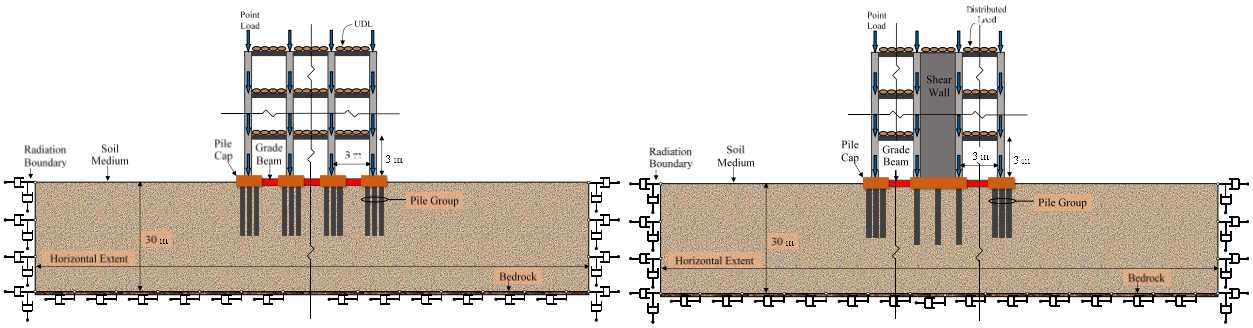

Figure 1. Illustration showing SSI model for (a) RC frame system and (b) RC wall-frame system.

2.1. Soil Profile

A cohesionless soil layer having a uniform depth of 30 meters is considered lying over an elastic bedrock. The choice of the depth of the soil layer is based on standard practice and guidelines for the characterization of soil profile outlined in seismic codes [34-35]. The basic properties of the different soil conditions considered are shown in Table 1. Namely four types of soil conditions have been considered representing (a) loose sand (S1), (b) medium sand (S2), (c) medium dense sand (S3), and (d) dense sand (S4). In cohesionless soil the response depends on the confining pressure developed at a given depth. For this it is essential to choose a model that is capable of simulating pressure dependent constitutive behaviour so as to ensure a proper confining action onto the pile foundations. Moreover, pressure

dependent behaivour is suitable for modelling a realistic shear wave velocity profile across the soil depth. Hence in the present study, 'PressureDependMultiYield' material model [36], that employs the nested yield surfaces [37-39] to simulate the failure criteria [40], has been utilized to model the soil [41], see Figure 2a. For hysteretic response under cyclic shear loads, the material model utilizes a purely kinematic deviatoric hardening rule [39, 42] as shown in Figure 2b. The octahedral stress-strain characteristic is represented by linearly approximating each yield surface interval as shown in Figure 2c. Twenty yield surfaces are employed in the present study for simulating the nonlinear constitutive behaviour of soil. The variation of the shear wave velocity across the depth of the soil domain is shown in Figure 3. It is worth mentioning that a soil domain with a nonlinear increase in the shear wave velocity across depth is a more realistic representation compared to the ones with constant or linearly increasing shear wave velocity. Further, it is to be noted that the adopted model for soil is an established one and has been used in several past studies [44-46]. The water table is assumed to lie at the bedrock level and is considered not to pose any influence onto the overlying soil.

Table 1. Basic properties and constitutive parameters of the soil.

Type of soil Condition	ρ (t/m^3)	φ (°)	ν	v_s (m/s)	G_r (kPa)	γ_{max}	d	Φ_T (°)
Loose (S1)	1.7	29	0.33	193	5.5×10^4	0.1	0.5	29
Medium (S2)	1.9	33	0.33	212	7.5×10^4	0.1	0.5	27
Medium dense (S3)	2.0	37	0.35	240	1.0×10^5	0.1	0.5	27
Dense (S4)	2.1	40	0.35	270	1.3×10^5	0.1	0.5	27

Note: ρ is the mass density of the soil, φ is the friction angle, ν is the Poisson's ratio, $v_s = \sqrt{G/\rho}$ is the average shear wave velocity, G_r and γ_{max} is the reference low strain shear modulus at and peak shear strain respectively at reference pressure $p_r^{'}$ = 80 kPa, d is defined by the relationship $G = G_r(p^{'}/p_r^{'})^d$, $p^{'}$ is the instantaneous effective confinement, G is the instantaneous shear modulus and Φ_T is the phase transformation angle.

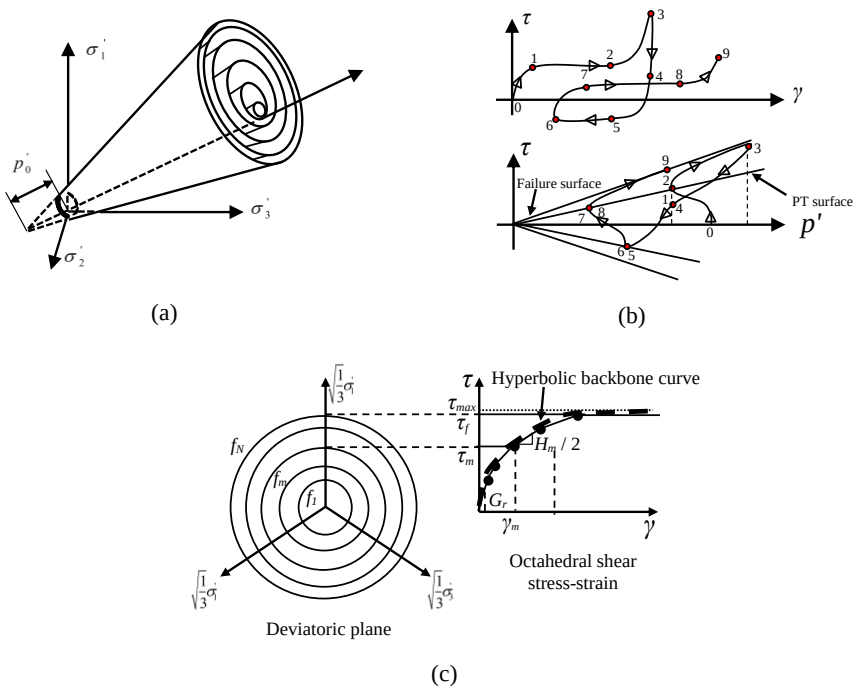

Figure 2. PressureDependentMultiYield material model [43]: (a) yield surface configuration in principle effective stress space (b) shear stress-shear strain curve and effective stress path, and (c) hyperbolic backbone curve and its piecewise-linear representation for the octahedral stress-strain response [37, 39].

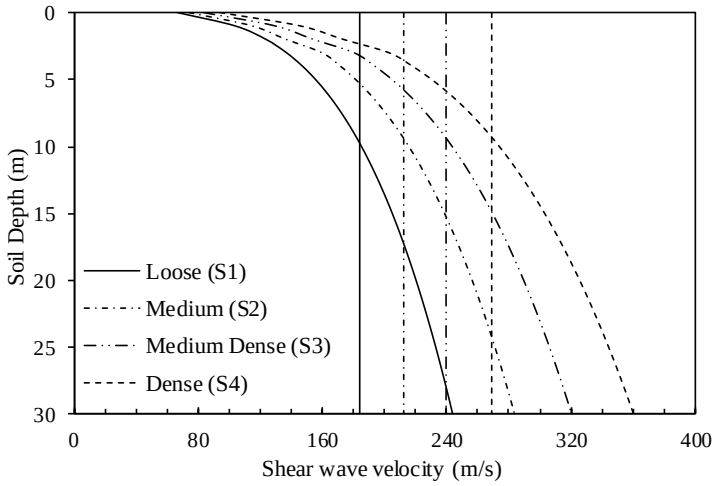

Figure 3. Shear wave velocity distribution across the depth of the soil considered.

2.2. Super-structure and Pile Foundation

Two types of systems, namely, (a) RC frame and (b) RC wall-frame have been considered in the present study. The storey height, as well as the bay width, are considered to be equal to 3 m. Each of the RC frame and RC wall frame systems are analyzed for different heights, i.e., (i) 9 m (3 stories), (ii) 18 m (6 stories), (iii) 27 m (9 stories), and (iv)

36 m (12 stories). Corresponding to a particular height of the system, different structural widths (number of bay) are considered, i.e., (i) 9 m (3 bays), (ii) 15 m (5 bays), (iii) 27 m (9 bays), and (iv) 45 m (15 bays). To represent the system type, height, and width of the specimen (in the mentioned order), an alpha-numeric nomenclature is used. For example, to label an RC frame system possessing 6 storeys and 15 number of bays, the nomenclature F6-15 is used. Similarly, the label W12-9 indicates an RC wall-frame system possessing 12 storeys and 9 bays. Representative illustration of the considered RC frame and RC wall-frame specimens is shown in Figure 4. Each of these configurations are considered to be supported by four different soil types (viz., S1, S2, S3 and S4) for which the superstructure design remains the same while the pile foundation design is modified as per the supporting soil type. Additionally, one fixed base condition (FB) for each configuration is also analyzed.

To design the RC frame and RC wall-frame systems relevant Indian Standards have been used. The intended use of the RC buildings is assumed to be for residential purposes and IS 875 Part 2 [47] has been used to estimate the gravity load, super-imposed dead load (3 kN/m^2), and the live load (3 kN/m^2). To represent the weight of unreinforced brick masonry infill wall, a uniformly distributed load having a magnitude of 5 kN/m is imposed onto the beams of the frame and wall-frame systems. The provisions of IS 1893 Part 1 [24] have been used to estimate the seismic forces on the superstructure systems by assuming that they are to be located in Zone V as per the Indian Seismic Zoning map. Further, IS 456 [48] and IS 13920 [49] have been utilized for designing the frame and shear wall sections subjected to the estimated gravity and seismic loads. The specification of the designed cross section of the members (column, beam and shear wall) are varied across the height of the superstructure as per the design requirements. It is worth mentioning that the difference between the frame and wall-frame system lies in the central bay, wherein a shear wall is incorporated which is being supported by a pile group system different from that of the columns (see Figures 1a and 1b).

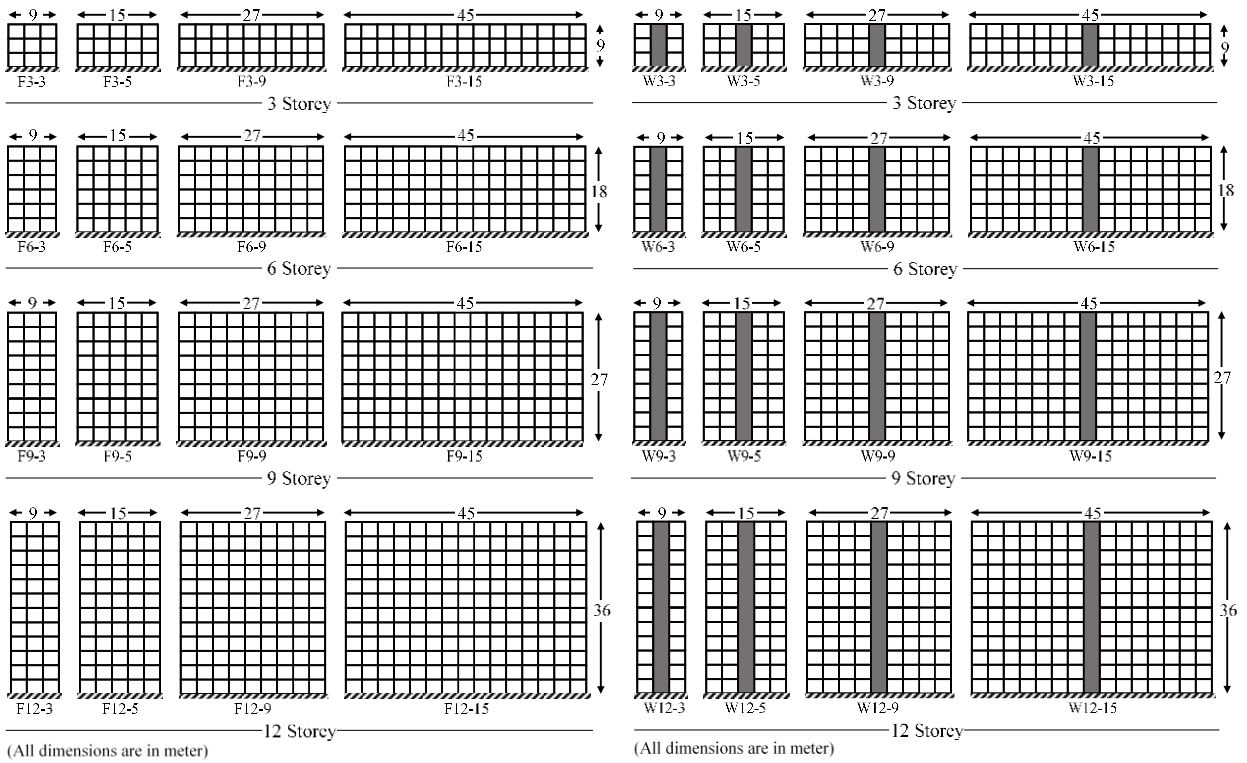

Figure 4. Configurations considered in the present study.

After estimating the gravity and seismic loads at the base of the superstructure system, the same have been utilized for designing the pile foundations as per the provisions of IS 2911 Part 1/Sec 1 [50]. Each column is supported by a group of 3 piles whereas the shear wall is supported by a group of 6 piles for all the specimens. As per the practice, the distance between the adjacent piles, in a pile group under the columns, is kept to be three times the diameter of the individual pile. For the purpose of design, M30 and Fe500 grade have been used for concrete and rebar, respectively, and the modulus of elasticity is estimated as given in IS 456 [48]. The cross-sectional details of the superstructure elements (beam, column and shear wall) and pile foundation are provided in Annexure A.

2.3. Idealization for Inelastic Behavior in the Super-structure and Pile Foundations

The superstructure and pile foundation elements have been discretized using beam-column elements, with each node possessing two translational and one rotational degree of freedom. Moreover, the equivalent frame method [51] has been adopted for modelling of the shear wall elements. The cross-section of each of the members is modelled into a number of fibers representing steel rebar and concrete, and the fibers are assigned with their respective uniaxial constitutive behavior. The constitutive relationship proposed by Menegotto and Pinto [52] and modified by Fillippou et al. [53] is used for simulating the uniaxial stress-strain characteristics of steel rebars (Figure 5b), and is employed

using the material model 'Steel02' available in OpenSEES. For concrete inside the core of a section, it is essential to capture the increase in strength and ductility as a result of the confining action imparted by the stirrups under axial loads. The cover concrete, on the other hand, can be modeled in an unconfined manner. In the present study, Kent-Park model [54] is used for the modelling the uniaxial stress-strain behaviour of unconfined concrete while modified Kent-Park model [55] is used for confined concrete (Figure 5a). The confined and unconfined constitutive behavior is employed in the numerical models with the help of the material model 'Concrete02' which is also available in OpenSEES. It is worth mentioning that the chosen models have been developed based on rigorous experimental studies and are widely implemented for simulating the nonlinear stress-strain constitutive behaviour of steel rebar and concrete [56].

In the superstructural members (beam, column and shear wall), the characteristics for possible inelastic behaviour are predefined at the two ends of each element by means of plastic hinges. Depending on the cross-sectional properties, the plastic hinge length in the beams and the columns is determined using the relationship proposed by Paulay and Priestley [23], as shown in Eq. (1).

$$l_p = 0.08l + 0.022 d_b f_y \tag{1}$$

In Eq. (1), l_p is the plastic hinge length (in m), l is the distance between the point of the maximum moment to the point of zero moment (in m), d_b is the diameter of longitudinal reinforcing bar (in m), and f_y is the yield stress of the reinforcement (in MPa). Similarly, the plastic hinge length in the shear wall is determined using the relationship proposed by Kazaz [57], and is expressed as:

$$L_p = 0.27 L_w \left(1 - \frac{P}{A_w f_c^{'}}\right)\left(1 - \frac{f_y \rho_{sh}}{f_c^{'}}\right)\left(\frac{M/V}{L_w}\right) \tag{2}$$

where L_p is the plastic hinge length of the shear wall, L_w is the length of the shear wall (in m), $P/A_w f_c^{'}$ is the axial force ratio (ratio of the axial load P to the load resisted by the concrete in the shear wall cross-sectional area, A_w), ρ_{sh} is the horizontal reinforcement ratio in the web of the shear wall and M / V is the shear span. For piles, the inelasticity is distributed over the entire length, since the equation for plastic hinge length in piles is not presently available in the literature. A perfectly bonded interface (PBI) model has been used for establishing node connectivity between pile and soil. A schematic representation of the PBI modelling approach is shown in Figure 6.

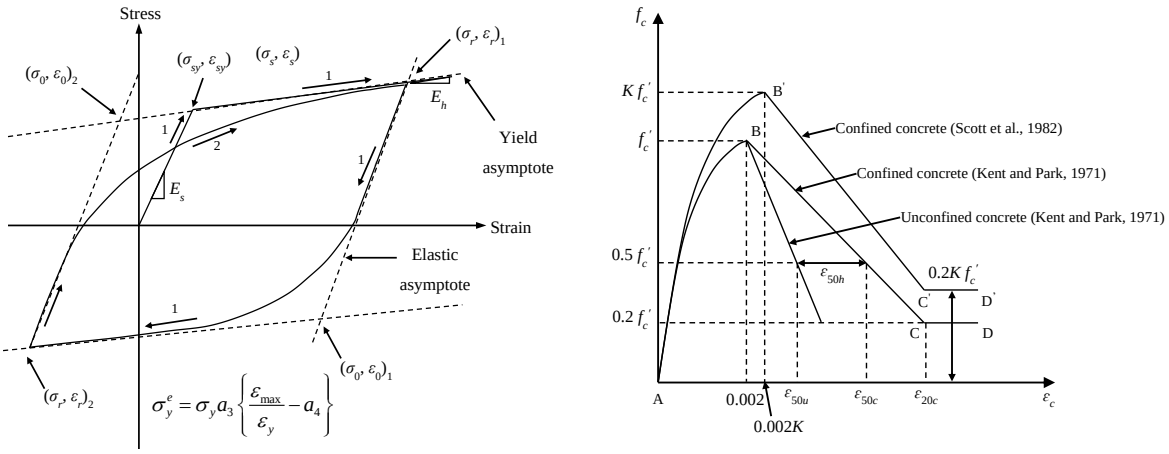

Figure 5. Uniaxial stress-strain models for (a) concrete and (b) steel rebar.

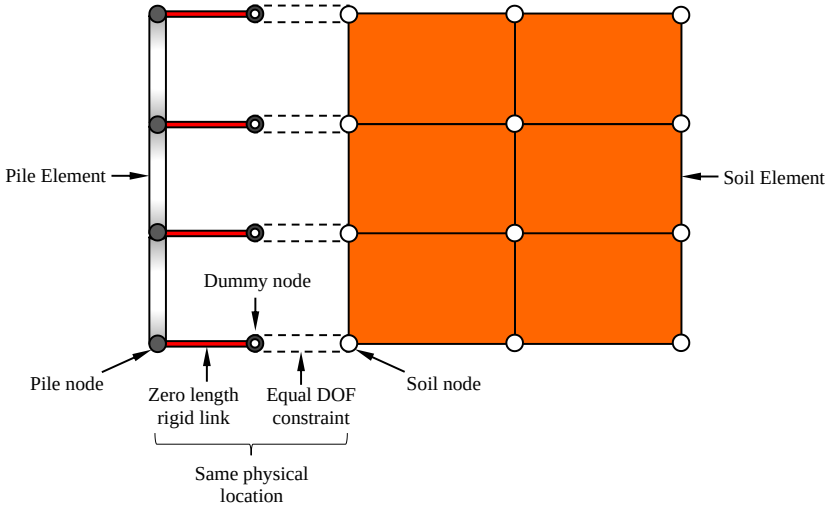

Figure 6. Representative illustration of the PBI approach for pile-soil interface modelling.

2.4. Boundary Condition, Element Discretization and Meshing Criteria

For SSI studies involving dynamic analysis, wherein it is essential to capture wave propagation accurately, radiation boundaries are utilized (shown in Figure 1) to represent the infinite soil domain extending in the horizontal and downward direction. The radiation boundaries usually employ viscous dashpots to eliminate artificial reflection of the seismic waves and ensure proper wave propagation phenomenon. In pushover analysis, however, the focus is on capturing the nonlinear response of the structural system under gradually increasing loads, rather than simulating dynamic wave propagation. Further, the viscous boundaries do not develop reactions in the case of static analysis as their behaviour is velocity dependent. Hence, displacement restrained boundaries are deemed appropriate for the present study. The horizontal basal boundary of the soil domain is restrained in the vertical and horizontal directions

whereas the vertical boundaries are restrained only in the horizontal direction and the vertical deformation of soil is allowed to simulate proper stresses under gravity loads. It is worth mentioning that utilizing restrained boundaries in case of nonlinear static analysis would not introduce inaccuracies in simulating realistic SSI behavior as long as the extent of soil domain considered is sufficient. To assure a minimal influence of the soil boundaries on the superstructure-substructure system, the prescription outlined by Sharma et al. [58] has been adopted for fixing of the lateral extent of the soil domain. According to the study, for any building with a particular width there exists an optimum lateral extent of soil domain beyond which the change in the overall response of the SSI system is insignificant. It is worth mentioning that the prescriptions were developed based on a dynamic analysis of the SSI systems. Utilizing these prescriptions for nonlinear static analysis would be more than sufficient as the extent of soil domain modeled is significantly larger than the influence zone of the soil-foundation system leading to the minimization of boundary effects. Hence in the present study, the width of the soil domain is determined based on the width of the frame configuration considered.

In finite element based numerical studies it is essential to ensure that the element discretization and meshing of the soil domain is appropriate. This ensures accurate results being captured through numerical simulation which is required to draw rigorous conclusions. The discretization of the soil domain has been carried out using four-noded bilinear isoparametric quadrilateral elements, possessing four gauss integration points. To arrive at an appropriate size of the mesh elements, convergence study is carried out by employing uniform sized elements having an aspect ratio of one. Several cases are examined wherein the mesh is progressively made finer and the change in the displacement of soil nodes under gravity load is observed. For example, Figure 7a shows the change in the displacement of the soil node underneath the central bay of the superstructure. It can be observed that as the mesh size is made finer, the change in the displacement diminishes and no further change is seen for a mesh element size fine than 0.5 m. Adopting this size for meshing would although produce accurate results, however, is quite expensive from the aspect of computational costs. Hence, an optimized structured non-uniform meshing (shown in Figure 7b) is adopted to ensure accuracy at low computational expenditures. A fine mesh element size of 0.375 m × 0.5 m has been adopted in the regions near to the structure-pile foundation system, while a coarse mesh element size of 1.5 m × 1.5 m has been considered in the regions far away from the system. To avoid interpolation error and severe mesh distortion during computation, it is essential to keep the aspect ratio within a safe limit. In this regard, the maximum aspect ratio of the elements has been limited to 4 [59]. It may be noted from Figure 7a that the adopted meshing scheme provides

sufficiently accurate results. It is worth mentioning that several past studies [60-63] on SSI have adopted a similar approach of employing the nonuniform meshing.

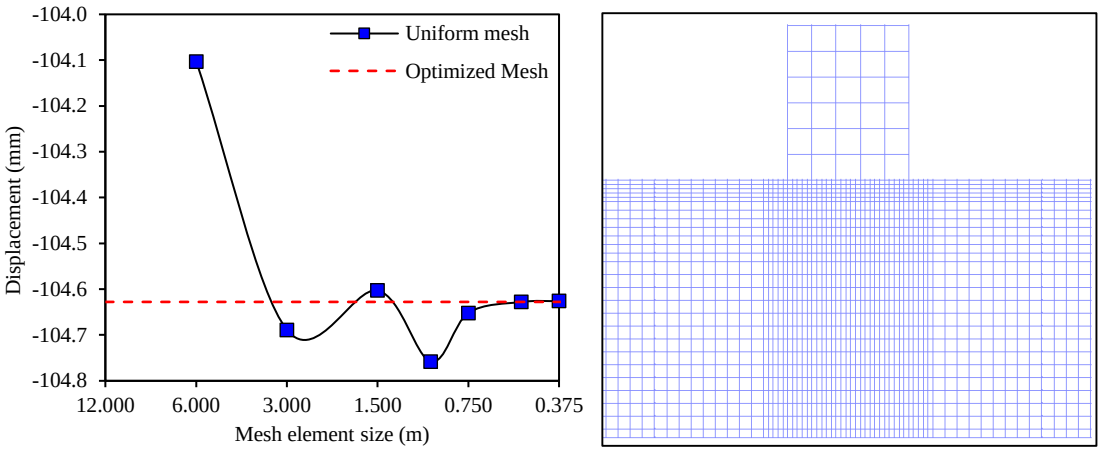

(a) (b)

Figure 7. (a) Mesh convergence study and (b) adopted non-uniform optimized meshing.

2.5. Validation of Numerical Modelling

Before proceeding to the detailed analysis, it is essential to verify that the adopted numerical modelling approach is capable of providing reliable results. In the present study, the modeling of the soil domain is validated by comparing the numerical estimates of the fundamental period (T_s) of soil domain under elastic condition with the theoretical values obtained from the expression shown in Eq. 3 [64].

$$T_s = 4.48\frac{D_s}{v_{sD}} \tag{3}$$

In the above equation, v_{sD} is the shear wave velocity of the soil corresponding to the depth of the soil domain considered (D_s). It can be observed from Figure 8a that there exists a sound agreement between the estimates form the two approaches with a maximum difference of less than 8%. Further, the ability of the soil domain to simulate dynamic response is tested by subjecting it to a sine wavelet and noting the peak total acceleration response across the depth of a soil column located at the center of the soil domain. A close agreement between the simulated results and those existing in literature [65] can be observed from Figure 8b.

Apart from the soil domain, it is also essential to ascertain the suitability of the selected material models to simulate the nonlinear behaviour in the structural members. For this, the nonlinear backbone pushover curve of an isolated column (3.25 m height) is compared with the results produced by Ko and Phung [66] in Figure 8c. Similarly,

the simulated nonlinear backbone pushover curve of an isolated shear wall (3.65 m height) is compared with the test results obtained by Thomsen and Wallace [67] and is shown in Figure 8d. It can be seen that the nonlinear behaviour of the members is satisfactorily simulated and hence the adopted modelling approach can be used for further analysis. For the sake of brevity, the member details as well as the loading information has not been reproduced here; they can be found in the cited references.

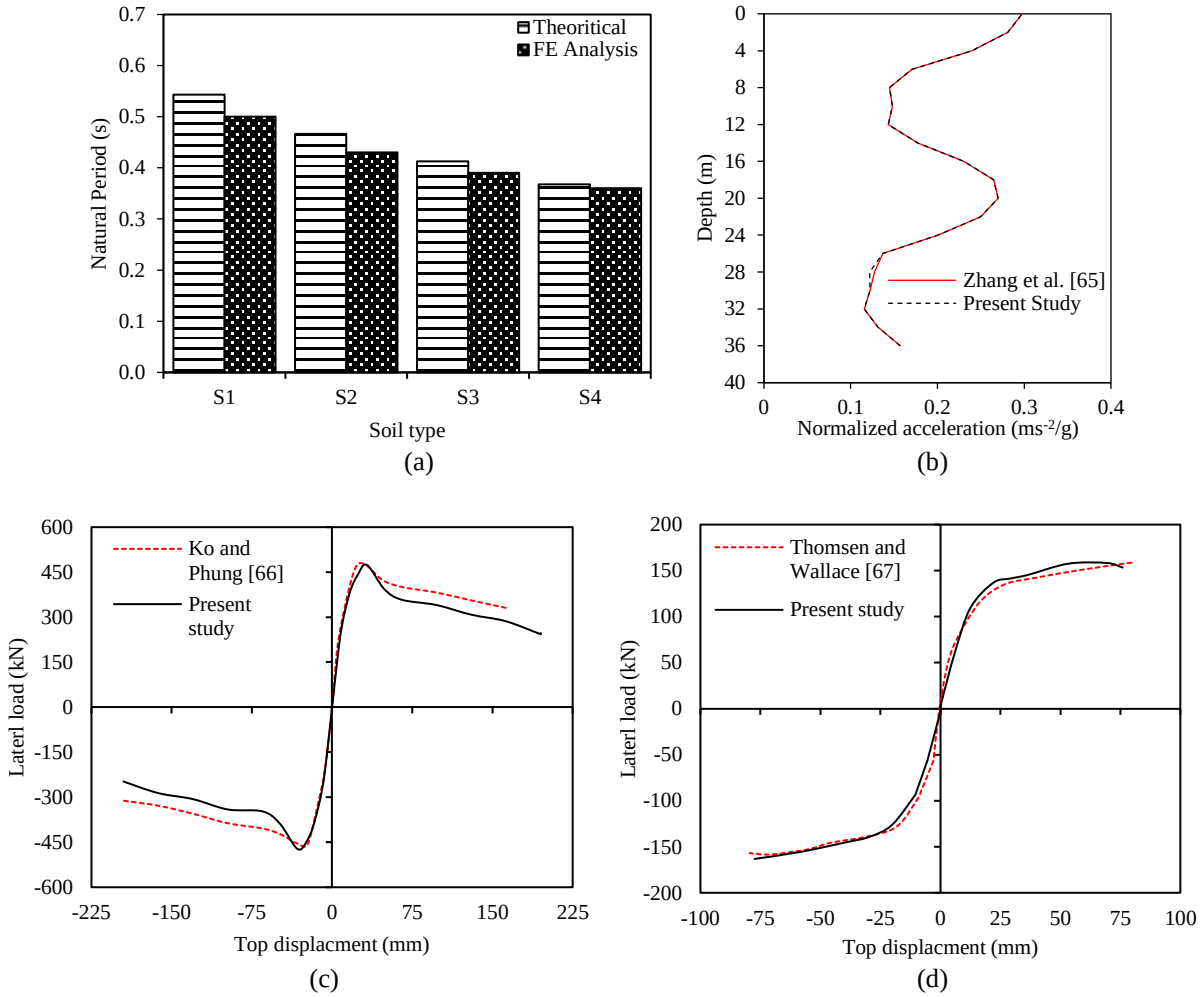

Figure 8 Comparison of results simulated in the present study for validation with those available in literature for (a) natural period of free field soil domain corresponding to the considered soil types (b) maximum acceleration response of soil column located at the center of a free field soil domain (c) nonlinear backbone pushover curve of RC column and (d) nonlinear backbone pushover curve of RC shear wall.

3. METHODOLOGY FOR ASSESSING INELASTIC BEHAVIOUR AND DUCTILITY CAPACITY

The methodology used for assessing the inelastic behaviour and ductility capacity of the RC frame and RC wall-frame systems with SSI effects is shown in Figure 9. Based on the modelling approach outlined, the SSI and fixed base (FB) models are created. These models are first subjected to a stage-wise static gravity analysis [65,68-69] in order to ensure that a proper static stress state and confining action is developed onto the piles. Next, Eigen analysis is performed to obtain the fundamental mode shapes of the SSI and FB models. These mode shapes are utilized as the lateral load distribution profiles while performing the displacement controlled nonlinear static pushover analysis in the subsequent stage. The outcome of the nonlinear static pushover analysis is obtained as roof drift (Δ, i.e., roof displacement measured from the base and normalized with respect to the height of the superstructure) versus the shear force developed at the base of the superstructure (V). The ultimate drifts are obtained by evaluating the performance state based on the inter-storey drift limits as prescribed in codal guidelines [70-71] and used in past studies [28-29]. Table 2 shows the various interstorey drift limits corresponding to the three different levels of damage states for the different types of vertical RC elements of the structural systems considered. It is worth mentioning that for buildings, IS 1893 Part 1 [24] prescribes an interstorey drift limit of 0.4% under design lateral load and no prescription is made for the evaluation of various inelastic performance states.

Table 2. Drift deformation limits as provided by FEMA-356.

Element type	Performance levels		
	Immediate occupancy (IO)	Life safety (LS)	Collapse prevention (CP)
Column frames	1%	2%	4%
Concrete walls	0.5%	1%	2%

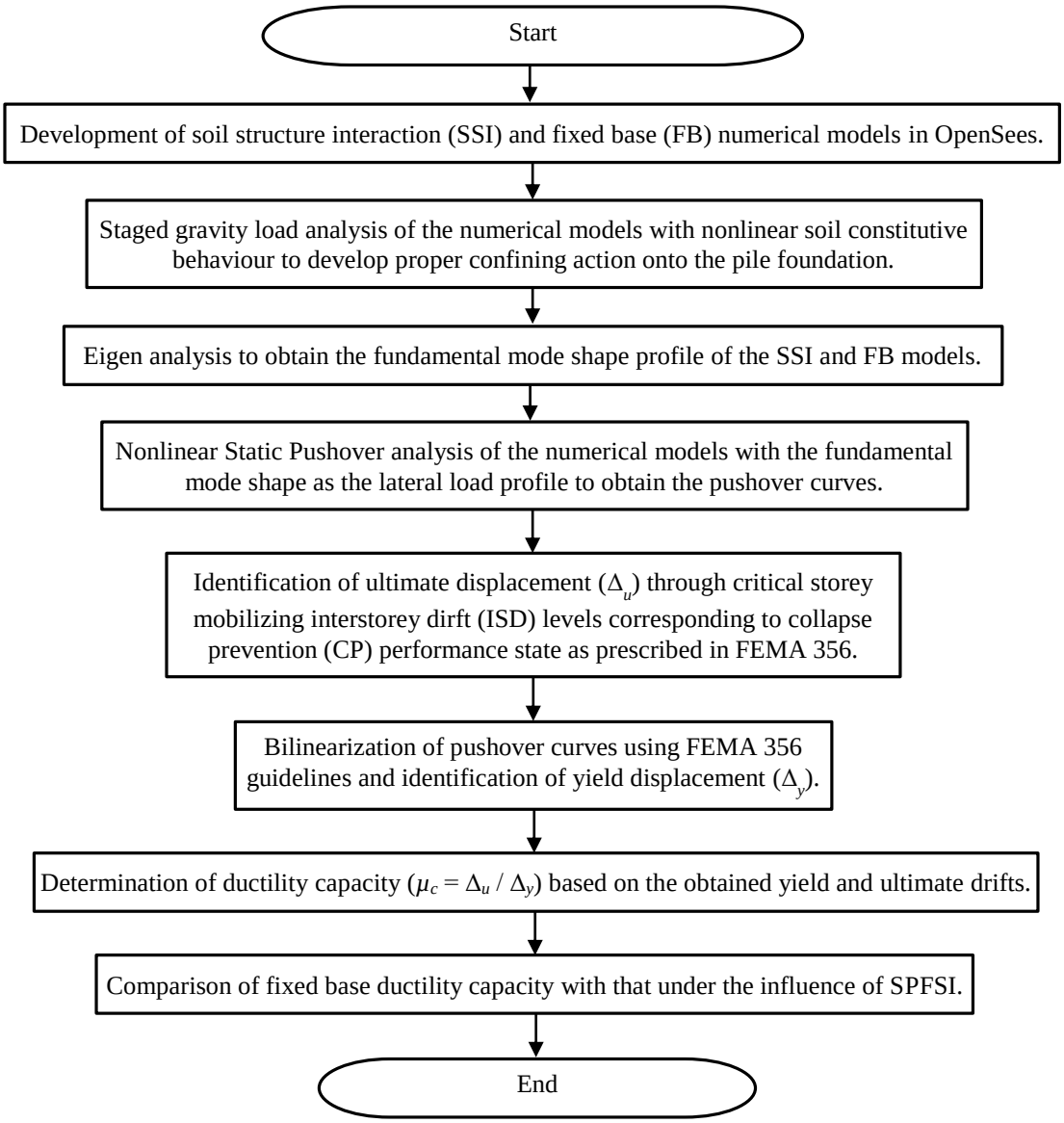

283

284 **Figure 9.** Methodology adopted for assessing inelastic behaviour and ductility capacity of RC buildings under SPFSI
285 and FB conditions.

286 For RC frame systems, the columns act as the primary lateral load resisting elements and their performance is very
287 much dependent on these elements. Similarly, in RC wall-frame systems, the damage incurred in the structural wall
288 (which bears a large share in the lateral load resistance) significantly affects the global performance. Hence, for RC
289 frame and RC wall-frame systems the collapse prevention (CP) limits corresponding to concrete frames and concrete
290 walls have been respectively utilized for identifying the ultimate state (i.e., Δ_u and V_u) in the pushover curve. Further,
291 the identification of the yield state (i.e., Δ_y and V_y) is done by bilinearizing the actual pushover curves using the

guidelines provided in FEMA 356 [71]. According to the guidelines, the initial and post-yield slopes (K_e and αK_e) are iteratively determined, so that two criteria are simultaneously satisfied, i.e., (i) the area above and below the actual curve is approximately balanced by the idealized pushover curve, and (ii) the initial stiffness of the idealized curve is set to match the secant stiffness of the actual pushover curve at $0.6V_y$. The process of bilinearization of the pushover curve (summarized in Figure 10a) begins by taking an informed guess of the yield values. The degree of satisfaction of the two criteria is checked with the guess values. Usually, the first set of guess values are chosen to be lower than the values expected to satisfy the criteria and hence the criteria is rarely satisfied in the first trial. Subsequent guesses are made by systematically increasing the guess value till both the criteria are satisfied. Figures 8b and 8c show the bilinear idealization of representative pushover curves having positive and negative post-yield slope respectively. Once the ultimate and yield drifts are obtained, the global ductility capacity of the structural system is obtained ($\mu_c = \Delta_u / \Delta_y$) for further analysis.

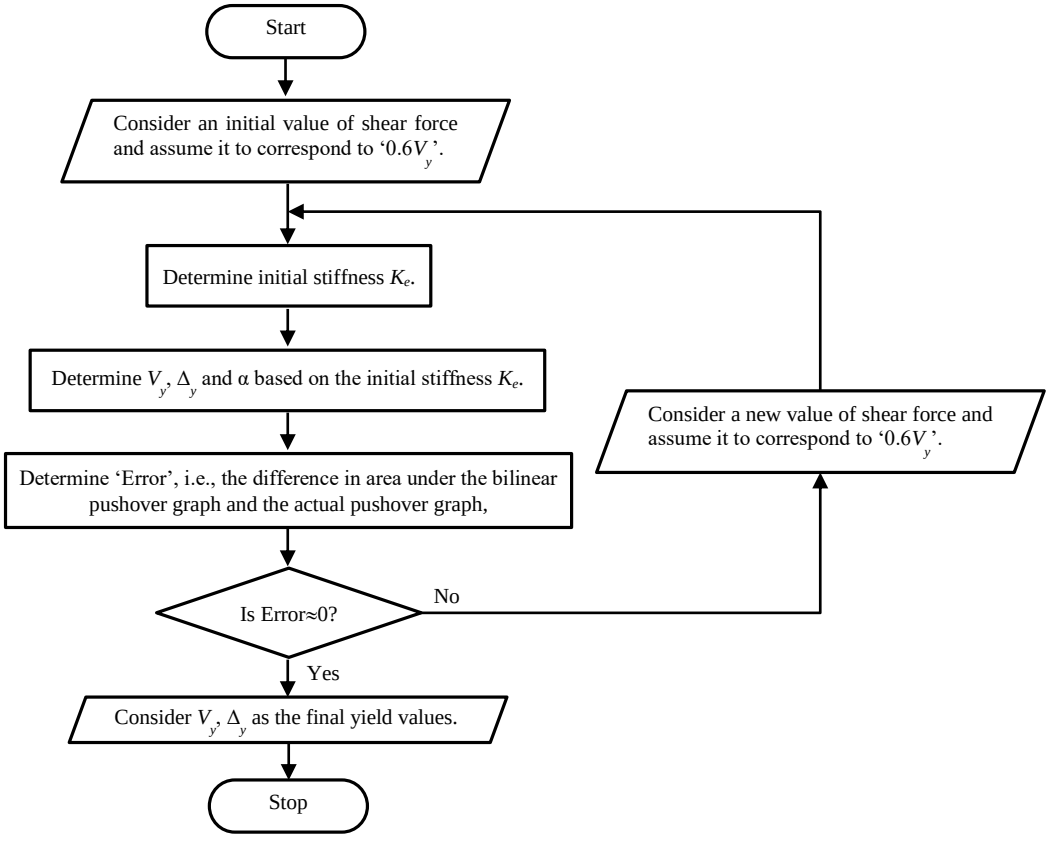

(a)

(a)

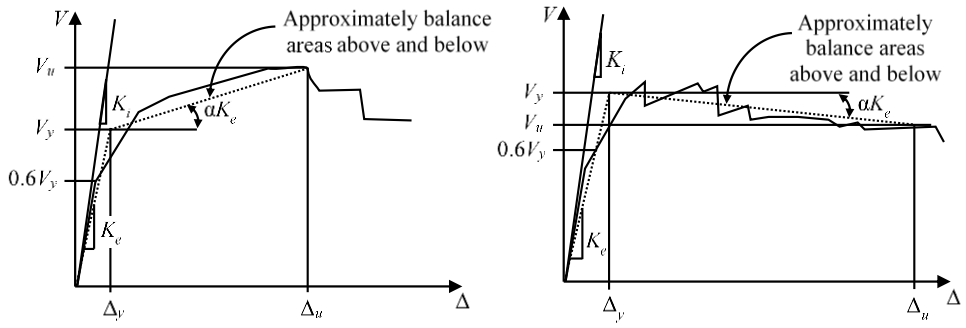

Figure 10. (a) Bilinear idealization process of pushover curves. (b) Bilinear idealization of representative pushover as per FEMA 356 for (a) positive post-yield slope, and (b) negative post-yield slope.

4. RESULTS AND DISCUSSION

4.1. Effect of SPFSI on Inelastic Super-Structural Response

4.1.1. Influence on base shear

The fixed base natural period of the different configurations of RC frame and RC wall-frame systems considered is shown in Figure 11. For a particular configuration, the fixed base natural period of RC wall-frame system is lower owing to its higher stiffness due to the presence of shear wall. The incorporation of SSI leads to modification in the natural period and the vibrational mode shape of the buildings. The mode shapes of the RC frame and RC wall-frame systems under SSI are shown in Figures 12a and 12b respectively. It can be observed that SSI leads to larger deformability in the building systems especially towards the lower storey levels wherein the effect of soil-pile foundation flexibility is greater. Also, the effect is much greater for the RC wall-frame systems as they are stiffer in comparison to RC frame systems.

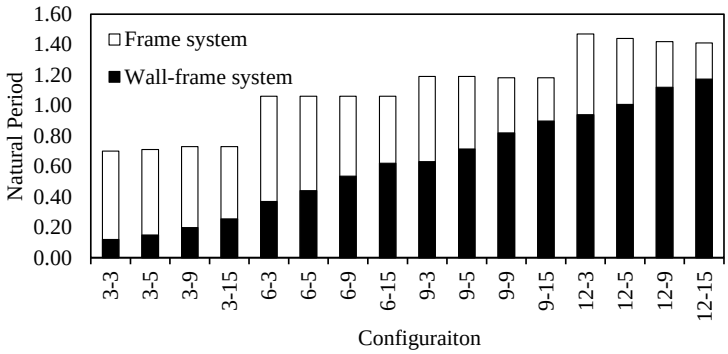

Figure 11. Fixed base natural period of the RC frame and RC wall-frame systems considered (*x*-axis indicates configuration, i.e., number of storeys and number of bays).

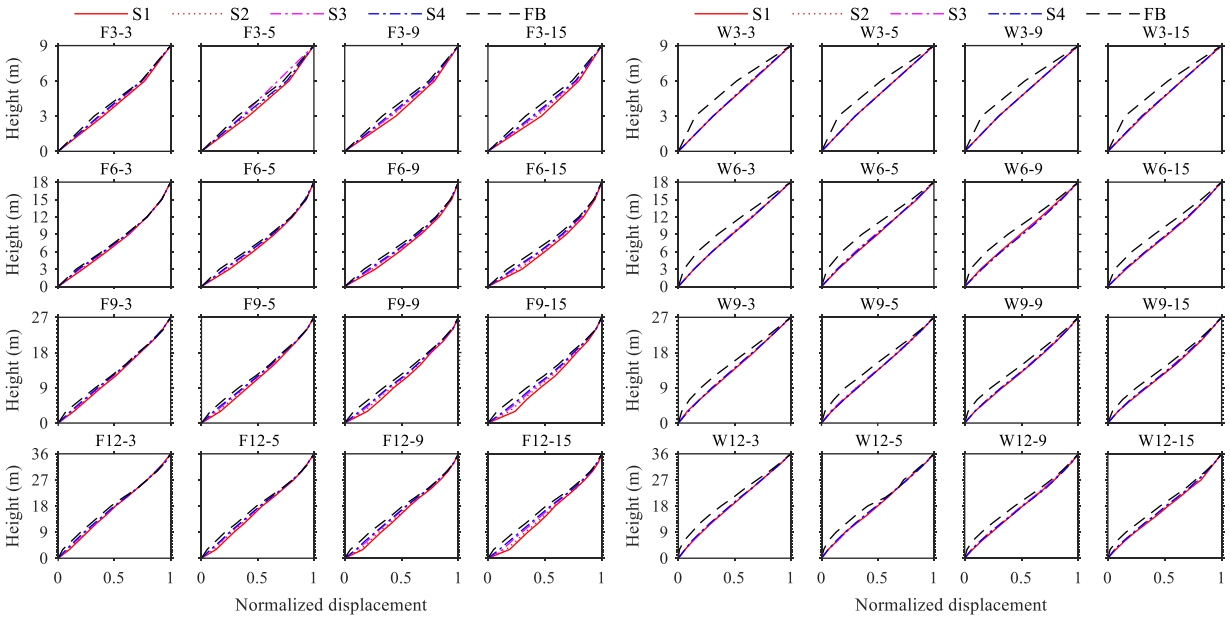

Figure 12. Influence of SPFSI on the fundamental mode shape of (a) RC frame systems and (b) RC wall-frame systems.

The pushover curves of the RC frame and RC wall-frame systems under the different support conditions are shown in Figures 13a and 13b respectively. It can be observed that the base shear developed in RC frame system is lower than that of the RC wall frame systems. Moreover, it can be observed that for RC frame systems the influence of SSI on the maximum base shear is marginal, and its magnitude for the SSI-incorporated case does not vary significantly from that of the fixed base (FB) case. The RC wall-frame systems on the other hand exhibited a greater change in the base shear under SSI effects. This is due to the presence of stiff shear wall which induces larger deformations at the base of the superstructure. Almost all the RC wall-frame configurations supported by S1 soil have the lowest base shear capacity, while those with FB condition exhibit the highest magnitudes. This is obvious since for the FB condition, it is expected that the structural system will attract larger forces as compared to that under the SSI cases. Moreover, the variation in V_{max} is observed to be the largest for W3-3 (most stiff RC wall-frame system) and least for W12-15 (most flexible RC wall-frame system). Additionally, for a fixed height of the wall-frame system, V_{max} reduces upon increasing the width from 3 bays (relatively stiff) to 15 bays (relatively flexible). This indicates that the effect of incorporating soil-foundation flexibility is more influential for a stiffer system. This is because stiffer systems (like W3-3) tend to attract greater inertial forces and moments onto the foundation, making them more sensitive to the flexibility introduced by the soil-pile foundation system. In the case of more flexible systems (like W12-3), this

tendency to attract high amounts of inertial forces and moments is less which consequently leads to a reduced impact of soil-pile foundation flexibility on the overall base shear. It is worth highlighting that the implication of such a change could be significant for the pile foundations. Large deformations induced on the pile foundation by stiff superstructural systems could increase rocking (discussed in Section 4.2) and inelastic rotations in the piles. Consequently, it would be suitable to design the piles under the influence of SSI with greater amount of reinforcement.

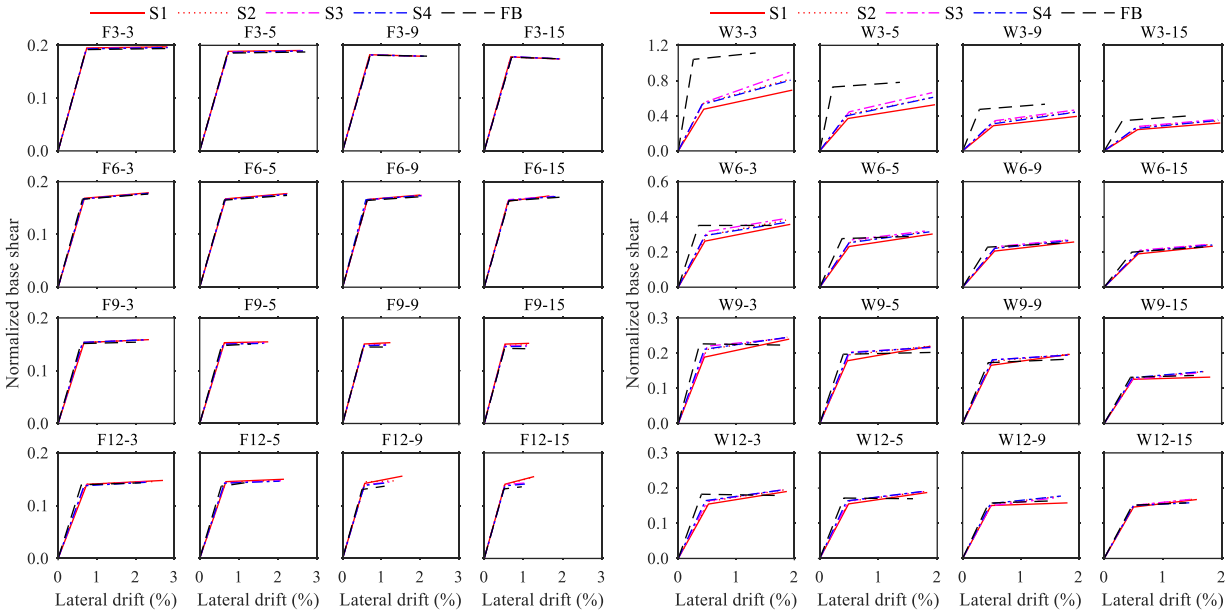

Figure 13. Influence of SSI on the inelastic behavior shown in the form of pushover curves for (a) RC frame systems and (b) RC wall-frame systems.

4.1.2. Influence on yield and ultimate drifts

From Figure 13a, it can also be observed that the variation in the yield drift (Δ_y) and ultimate drift (Δ_u) is quite insignificant for RC frame systems. It is however noted that in case of short frames (3 and 6 storey), Δ_u for the FB case is relatively larger compared to that obtained for the SSI cases. For the taller RC frame systems (9 and 12 storey), the trend is interestingly reversed, wherein Δ_u is relatively lesser for FB case. For instance, under FB condition, Δ_u for F3-15 is 2.01, while that for S1 soil condition is 1.92; on the other hand, Δ_u for F12-3 under FB condition is observed to be 2.14 which is correspondingly increased to 2.69 under S1 soil condition. The reason for the foregoing observations can be understood by studying the interstorey drift (ISD) profiles of the frame systems as shown in Figure 14a. It can be observed that corresponding to most frame systems with small height (3 storeyed and 6 storeyed frames),

363 the development of peak ISD is at lowermost storey level. Moreover, for these frames the ISD profiles exhibit lower
364 values under the influence of SSI (lowest for S1). As SSI introduces flexibility at the superstructure base, the peak
365 ISD value is achieved at lower Δ_u for the frames under the influence of SSI. For taller RC frame systems (9 storeyed
366 and 12 storeyed frames), peak ISD develops at higher storey levels (L4 for 9 storeyed frames; L4 and L7 for 12
367 storeyed frames). When compared with the FB condition, the ISD profiles exhibit larger values under the influence of
368 SSI (highest for S1 soil type). Further, taller systems tend to exhibit rocking under the influence of SSI leading to the
369 development of larger deformations near superstructure base. The combined effect of soil-pile foundation flexibility
370 and the resulting rocking motion leads to larger overall deformations and consequently greater Δ_u for the SSI case.
371 For a fixed height of the frame, irrespective of the SPF case, increasing the frame width reduces the ISD values at
372 storey levels adjacent to the one where collapse is imminent due to the higher redundancy in wider frames and hence
373 leads to smaller Δ_u. For few frames (F12-3, F12-5, and F12-15), SSI causes a shift in the location of imminent collapse
374 developed at a particular storey. Hence, depending on the inherent behaviour and location where collapse criteria are
375 satisfied, the RC frame system may or may not exhibit larger ISD profile and consequently larger ultimate drifts (Δ_u)
376 under the influence of SSI.
377 For RC wall-frame systems, the variation in the yield drift (Δ_y) and ultimate drift (Δ_u) is quite evident for the
378 shorter configurations (relatively stiffer) and is reduced for the taller wider configurations (relatively flexible), as can
379 be observed from Figure 13b. Moreover, Δ_u is relatively higher for the SSI cases as compared to the FB case. The
380 rationale behind the observations can be understood with the help of the inter storey drift (ISD) profile for various RC
381 wall-frame systems shown in Figure 14b. For all the configurations it can be observed that the variation is not
382 significant towards the higher storey levels. However, due to the presence of soil-pile foundation flexibility and the
383 resulting tendency of the wall-frame system to deform more towards the base, at L1 the ISD for SSI case is higher
384 when compared to that of the FB condition (except for 9 storey wall-frame systems). This causes the wall-frame
385 systems to exhibit higher Δ_u under SSI. For 9-storeyed wall-frame systems, the variation in ISD at L1, for various
386 support conditions (SSI or FB), is observed to be very small due to a similar magnitude of inelasticity developed
387 within the system under the different SPF conditions. In some exceptional cases, larger ISD is observed for stiffer soil
388 types (e.g., for W12-9, at L1 level, ISD for S3 soil type is larger than that obtained for S2 soil type). Further, for a
389 particular height, configurations exhibiting larger ISD values at several storey levels exhibit greater Δ_u values (e.g.

the narrow configurations (3 bays and 5 bays) of 12-storeyed wall-frame systems under all SPF conditions). Thus, the ultimate drifts exhibited by RC wall-frame systems under SSI are greater than that observed under fixed-base condition due to significant increase of ISD at the bottom storey level.

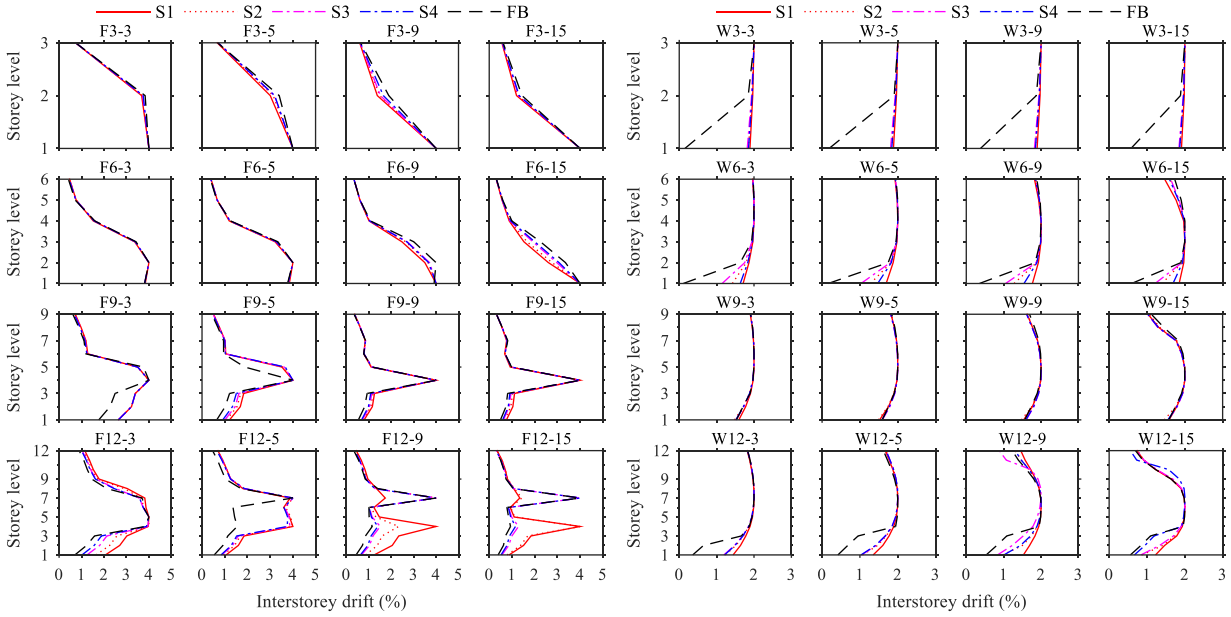

Figure 14. Influence of SSI on the inelastic behavior shown in the form of interstorey drift (ISD) profiles for (a) RC frame systems and (b) RC wall-frame systems.

4.2. Effect of SPFSI on Inelastic Pile Foundation Response

Foundation rocking is an important parameter that is influenced by the response of the soil-pile foundation system and at the same time influences the superstructure response. Under gravity loading, the forces transferred onto the columns of the superstructure and the pile groups are compressive in nature. Whereas under lateral loads half the columns develop compression while the other half develop tension as shown in Figure 15. The combined effect of gravitational and lateral loads leads to a variation in the compressive loads in the columns and the pile groups (some of the pile groups experience a reduction in the compressive forces while others experience an increase). This eventually influences the magnitude of rocking as well as the inelasticity developed in the piles. For RC frame systems, as shown in Figure 15, four groups of pile foundation are considered wherein two belong to the exterior most columns (‘E'’ with least compression and ‘E’ with the highest compression), and the other two belong to the innermost columns (‘I'’ with relatively lesser compression and ‘I’ with relatively higher compression). For RC wall-frame systems, instead of the two groups corresponding to the innermost columns, the pile group supporting the centrally located shear wall is

considered and is labelled as ‘W’. The rocking of the pile foundation groups embedded under different soil conditions for the various RC frame and RC wall-frame systems is shown in Figure 16a and 16b respectively. Further for each of the groups, the inelastic behaviour in the piles having the lowest and highest compression, labelled as ‘e'’ and ‘e’ respectively (see Figure 15), are examined. The plastic rotation at ultimate state developed in the piles of the critical groups are shown in Figure 17 for RC frame systems and in Figures 18-19 for RC wall frame systems. Further, the correlation of three important parameters in the pile groups of the frame and wall-frame systems are shown in Figure 20.

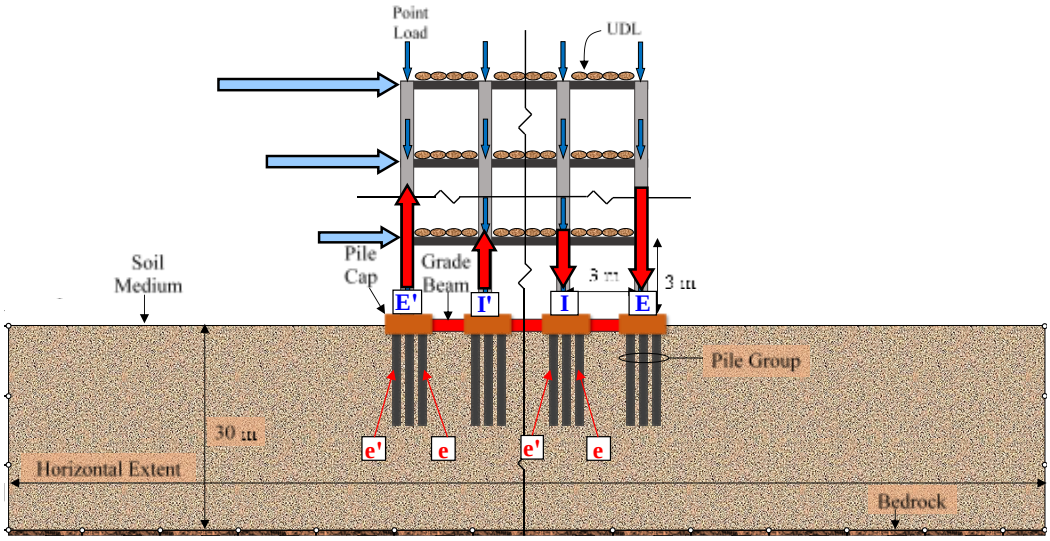

Figure 15. Schematic illustration showing the different pile groups and piles within a group examined in the study.

4.2.1. Role of compressive loads and soil

Under compressive loads, cohesionless soil develop confining action which affects the rocking of the pile group and the inelasticity developed in the piles. From Figure 16a, it can be observed that, pile group E', supporting columns with the least compressive loads, exhibits the largest rocking, while group E, under columns with greatest compression, shows the least. Further, pile groups I' and I display intermediate rocking, consistent with the magnitude of compressive loads they bear. The observation is due to the fact that greater the compressive loads greater is the confining action which tends to reduce the rocking in the pile group foundation. Further, the rocking of the pile groups I', I and E is greater for the weaker soil condition S1 due to the lesser confining action under compressive loads compared to the stiffer soil conditions (S2, S3 and S4).

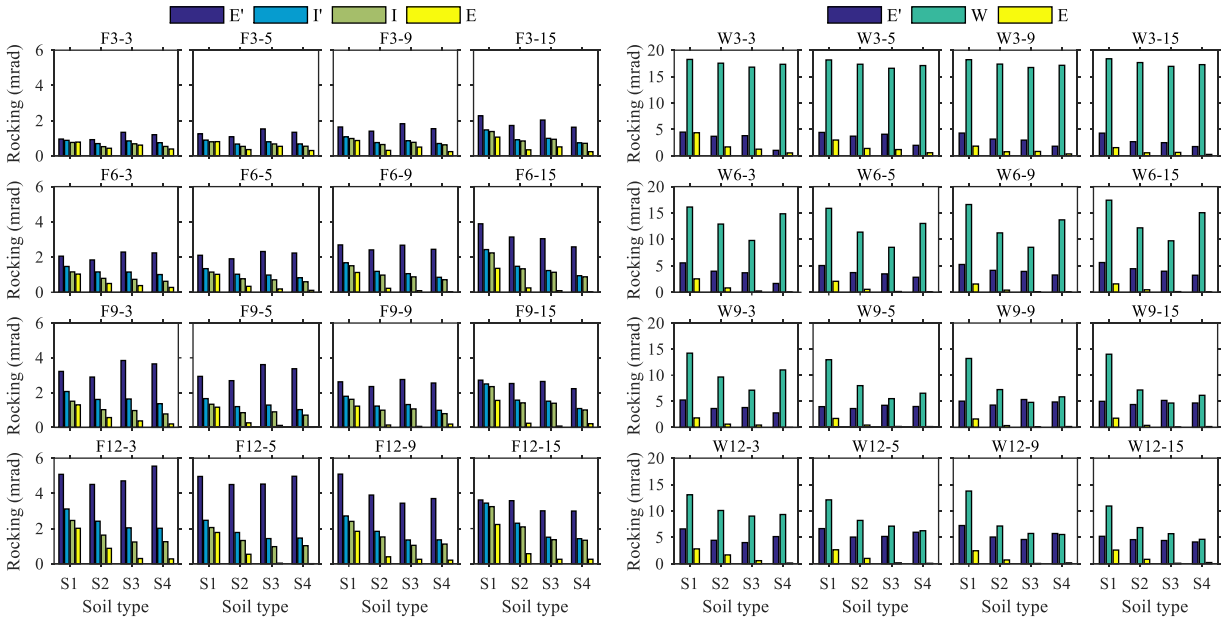

(a) (b)

Figure 16. Influence of SPFSI on pile group rocking for (a) RC frame systems and (b) RC wall-frame systems.

The confining action of the soil not only influences the rocking but also the inelasticity developed in the piles. It can be seen from Figures 17a and 17b that due to a greater confining action and reduced rocking in pile group E, the plastic rotation in the piles is also lesser compared to that of group E'. Additionally, for almost all the configurations, the piles embedded in S2, S3, and S4 soil exhibit significantly lesser plastic rotations as compared to that of S1 soil type. This is due to the confinement effect being larger for the stiffer soil types (S2, S3, and S4), thereby inhibiting the development of plastic rotations. It is worth noting that this effect is prominently visible for pile group E wherein the soil develops significant confining action owing to the presence of higher compressive loads.

4.2.2. Role of superstructure response

Under SPFSI effects, the inherent inelastic behaviour of the superstructure influences the foundation response. From Figure 16a it can be observed that for short RC frame systems (3-storeyed and 6-storeyed), the magnitude of rocking exhibited in the pile groups is larger corresponding to the wider configurations (9 bay and 15 bay). The is due to the superstructure meeting the collapse criteria with a relatively high ISD value near to the base causing higher rotation/rocking within the pile groups (see Figure 14a). For taller RC frame systems (9-storeyed and 12-storeyed), on increasing the width (from 3 bay to 15 bay), the magnitude of rocking for pile group E' reduces, whereas it increases for the other groups (E, I', and I). The explanation for this complex phenomenon is twofold. Firstly, for wider configurations, large ISD values tend to get concentrated at the level of imminent collapse which induces the frame

to achieve ultimate state at lower values of roof drifts thereby reducing the rocking of group E'. Secondly, the lower roof drifts resulting into a reduced compressive load and a limited spread in nonlinearity leads to an increase in transfer of lateral load at the base, hence, the combined effect causes an increase in the rocking of the other pile groups (I', I and E).

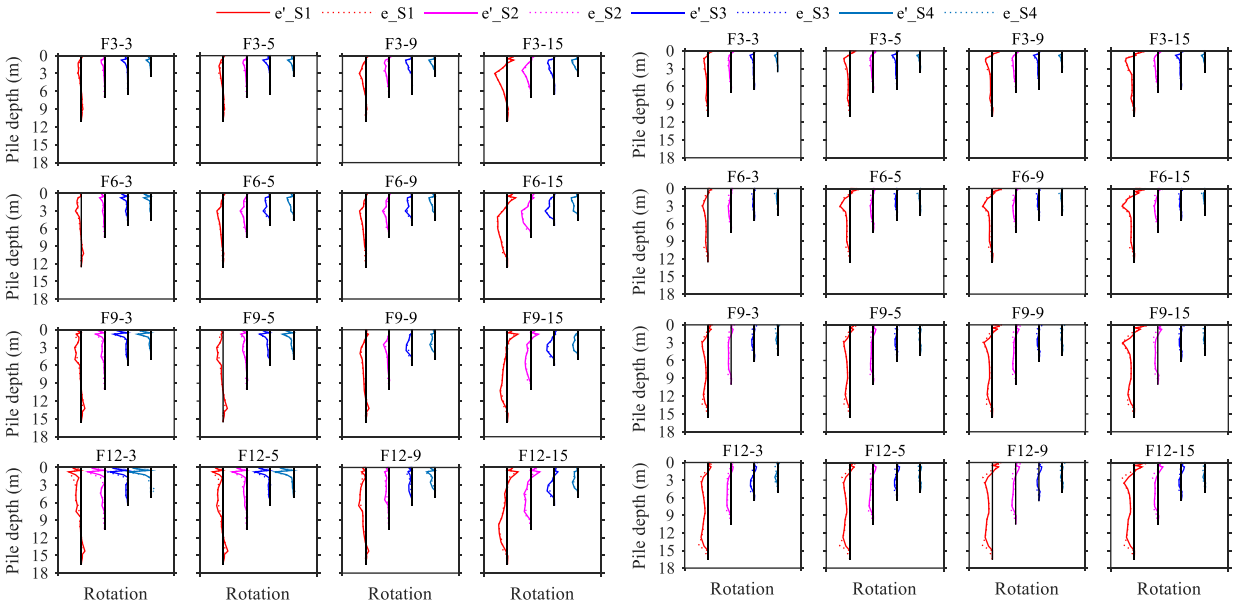

Figure 17. Influence of SPFSI on the inelastic rotation of piles belonging to group (a) E' and (b) E, for the various configurations of RC frame systems.

The rocking of pile groups is also influenced by the type of member supported by them. In the case of RC wall-frame systems (Figure 16b), it is observed that the pile group under the shear wall (W) exhibit significantly higher magnitude of rocking compared to that of the pile group under the columns (E' and E). This is because compared to the columns, the shear wall is a stiffer member and attracts larger forces and moments leading to a higher magnitude of rocking. Moreover, it can be observed that the magnitude of rocking is largest for the 3-storeyed wall-frame systems, and reduces as the height of the wall-frame system is increased. This is because the short wall-frame systems, being stiffer, attract greater base shear (Figure 13b). Further, upon increasing the width of the frame with a particular height, the magnitude of base shear developed by the wall-frame system is reduced. However, the magnitude of rocking of pile group W is approximately similar for the different widths of the wall-frame systems (e.g., 3-storeyed and 6-storeyed frames). Such an observation can be understood by relating the rocking with the similar magnitude of ISD developed at L1 (Figure 14b) corresponding to the different widths of the wall-frame systems. In the case of 9-storeyed

and 12-storeyed configurations, the reduced magnitude of rocking in group W under S4 soil can also be related to the lesser magnitude of ISD developed in the wall-frame systems at storey L1 (Figure 14b).

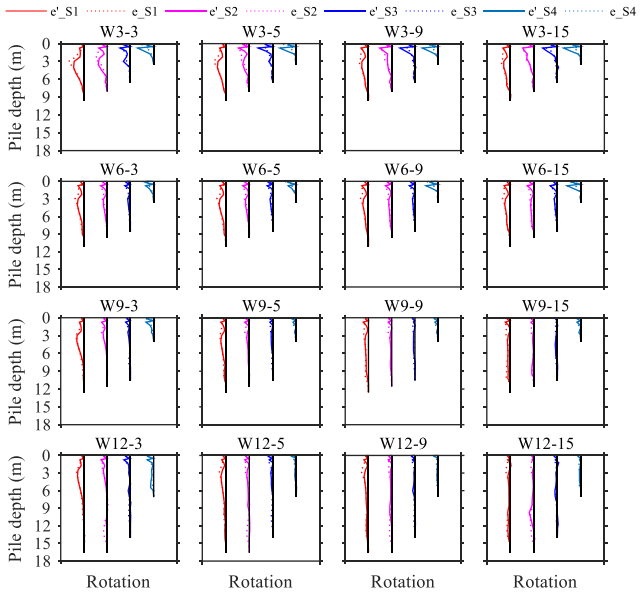

Figure 18. Influence of SPFSI on the inelastic rotation of piles belonging to group W for the various configurations of RC wall-frame systems.

The inelastic rotation developed in the piles can also be associated with the superstructure response. For e.g., in Figures 18 and 19, it can be seen that, similar to the observation made for rocking, the plastic rotation is also observed to be the highest for the piles corresponding to W3-3 due to the magnitude of base shear being highest for the system. On the other hand, the plastic rotation in the piles is least for W12-15 for which the magnitude of base shear is also the lowest. Similarly, for a particular soil type and height of the RC wall-frame system, the plastic rotation in the piles is reduced on increasing the width owing to the reduced magnitude of base shear.

4.2.3 Role of pile geometry

The geometry of the pile also influences the rocking and inelasticity in the pile group. For a number of cases corresponding to RC frame and RC wall-frame systems, the rocking exhibited by pile group E' under weaker soil (S1) is lower than that for the other relatively stiffer soil conditions (e.g., see F12-3 in Figure 16a and W9-9 in Figure 16b). This is because the piles are larger in length under softer soil conditions leading to higher embedment stiffness which may reduce the rocking tendency. Moreover, the piles embedded in stiffer soil possess smaller lengths and cross-sectional area which may lead to reduced stiffness and hence increased rocking. Under these circumstances, the piles

embedded in the stiffer soil exhibit larger plastic rotation near the top of the pile. Corresponding to pile group E larger rocking is observed if the piles exhibit significant plastic rotation along the length. For example, in the frame F9-15 under S1 (Figure 17b) the piles develop significant plastic rotation that is distributed over the length, thereby exhibiting a larger magnitude of rocking (Figure 16a) when compared with that of the frame F9-3. This observation is not noticeable for piles embedded in S2, S3, and S4 soil types owing to the larger confining action leading to a lesser rocking of the respective pile groups.

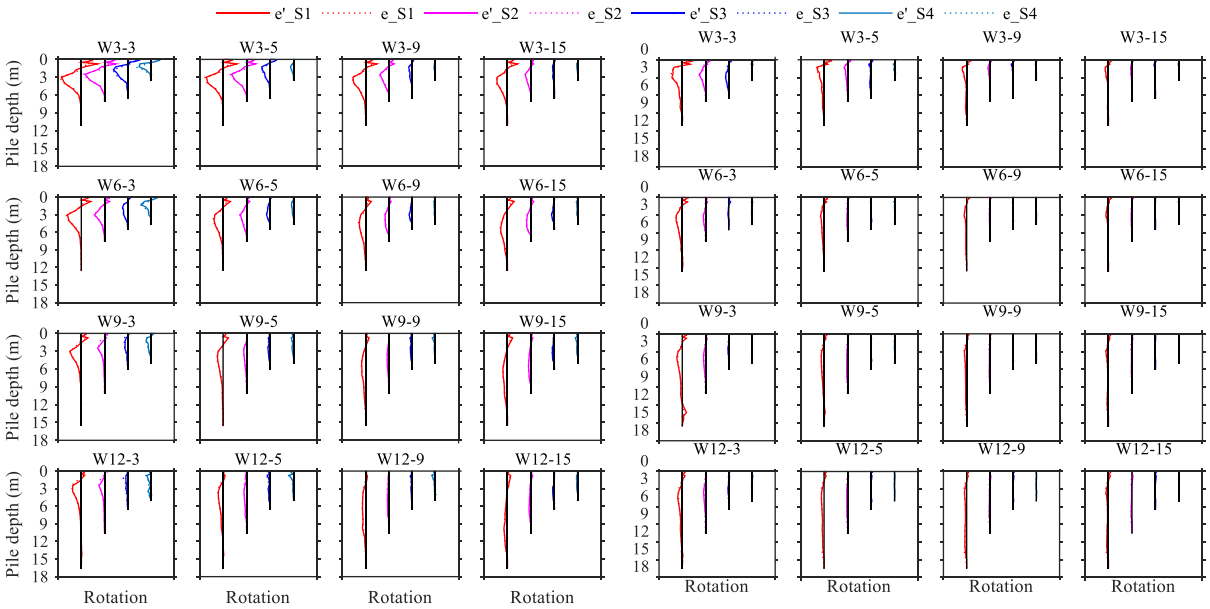

Figure 19. Influence of SPFSI on the inelastic rotation of piles belonging to group (a) E' and (b) E, for the various configurations of RC wall-frame systems.

4.2.4 Correlation between key parameters

Pearson correlation between the three key parameters, i.e. change in force (FR) due to lateral loads, rocking (RO) of the pile group and inelastic rotation (IR) developed in the piles is determined for RC frame and RC wall fame systems as shown in Figures 20a-20e. From Figure 20a, it can be observed that for RC frame systems, pile group E' showed positive correlation among these three parameters. This implies that pile groups on experiencing a reduction in the compressive forces experience an increase in rocking and inelastic rotations. Pile group E on the other hand showed no correlation between FR and RO and a low negative correlation between FR and IR. This is because pile group E experiences an increase in the compressive forces under which pile groups experience less rocking. At the same time,

an increase in compressive forces on the pile group causes the soil strength to increase thereby imparting a confinement effect on the piles and eventually reducing the inelastic rotation.

For pile group E' in the wall frame systems, while the correlation between FR and RO is positive, it is slightly negative between FR and IR. This is because, except for the 3 storey cases, in all others cases the pile groups experienced tensile forces. Piles groups experiencing tensile forces exhibit pull-out action onto the piles due to which the inelastic rotation is reduced. Moreover, due to the development of tensile forces, the inelastic rotation (IR) is fairly uncorrelated with rocking (RO). Pile groups E, in the wall-frame systems showed a slight negative FR-RO and FR-IR correlation due to an increase in the compressive loads. In the case of pile group W, as it is located centrally, the FR-RO and FR-IR correlation lies between that of pile group E' and E. The correlation between RO-IR in all the cases is positive except when tensile forces are encountered and the inelastic rotation is uncorrelated with rocking.

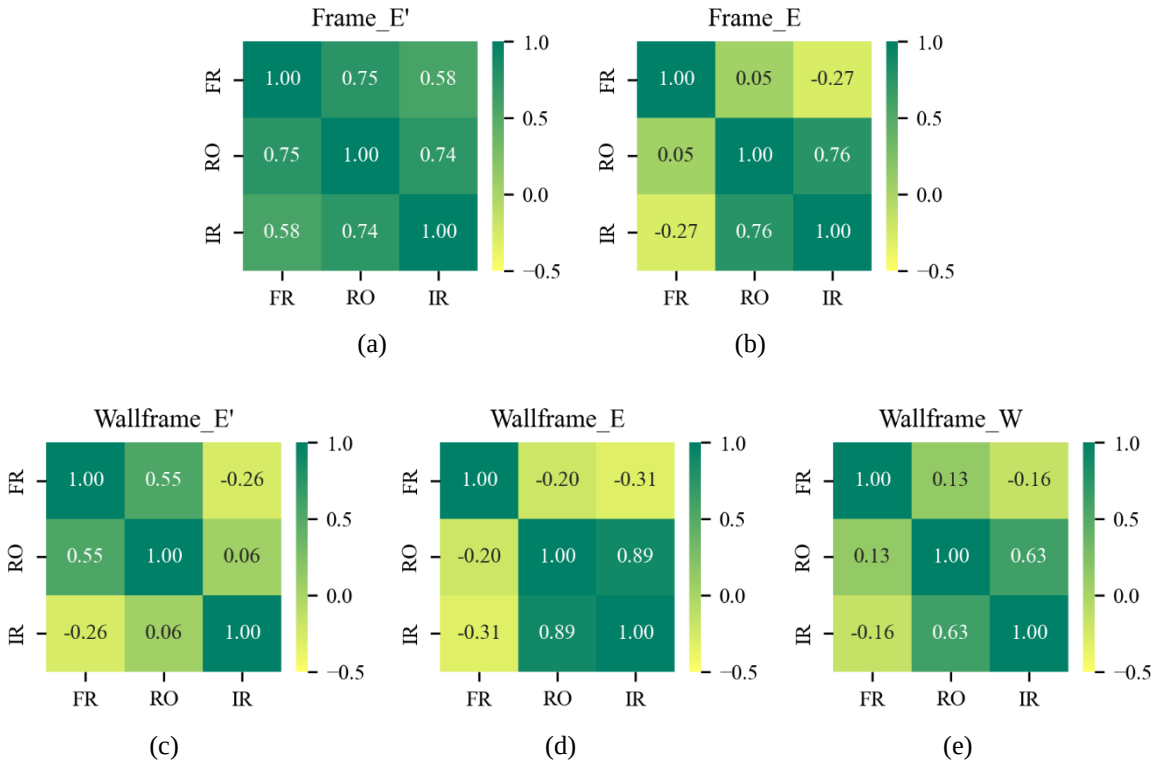

Figure 20: Pearson correlation coefficient and heat map for pile group (a) E' and (b) E of RC frame system; (c) E', (d) E and (e) W of RC wallframe system.

4.3. Influence of SPFSI on Ductility Capacity

As observed in the foregoing sections, the presence of soil-pile foundation system causes the plastic behavior of the superstructure systems to be different from its fixed-base behavior modifying the yield and ultimate drifts. As already

observed for RC frame systems the modification in yield drift (Δ_y) under the influence of SPFSI has been pretty insignificant while that for RC wall-frame systems has been observable. From Figures 21a-21d, it can be observed that the modification in the ultimate drifts (Δ_u) for RC frame system under SPFSI has been relatively less in 3, 6 and 9 storeyed frame systems as compared to the 12-storey frame system. Also, for shorter RC frame systems (3-storeyed and 6-storeyed frames), Δ_u under SSI is lower than that observed for the FB case, however, for taller RC frame systems (9-storeyed and 12 storeyed) the vice-versa is observed. Similarly, from Figure 22a-22d it can be observed that for all the RC wall-frame configurations considered, the SSI cases exhibit larger Δ_u compared to that obtained under the FB case (except for W9-3, W9-5, and W9-9 for which Δ_u under the SPFSI and FB cases are similar). Moreover, the increase in Δ_u under the influence of SPFSI is the largest for 3-storeyed wall-frame systems and least for 9-storeyed wall-frame systems. The modifications in the yield and ultimate drifts can be categorized in the following four scenarios, viz., (I) reduction in Δ_u with an insignificant change in Δ_y, (II) increase in Δ_u with an insignificant change in Δ_y, (III) increase in Δ_y with an insignificant or significant change in Δ_u. Scenarios (I) and (III) lead to a reduction in the ductility capacity ($\mu_c = \Delta_u / \Delta_y$) while scenario (II) leads to an increase. The modification in the ductility capacity of RC frame and RC wall-frame systems is discussed with respect to these scenarios in the following sections.

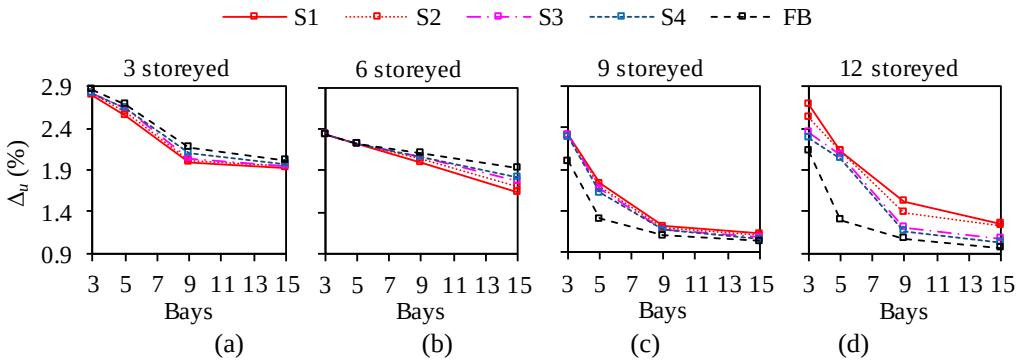

Figure 21. Influence of SPFSI on ultimate drift of RC frame systems of different width and height of (a) 3 storey, (b) 6 storey, (c) 9 storey and (d) 12 storey.

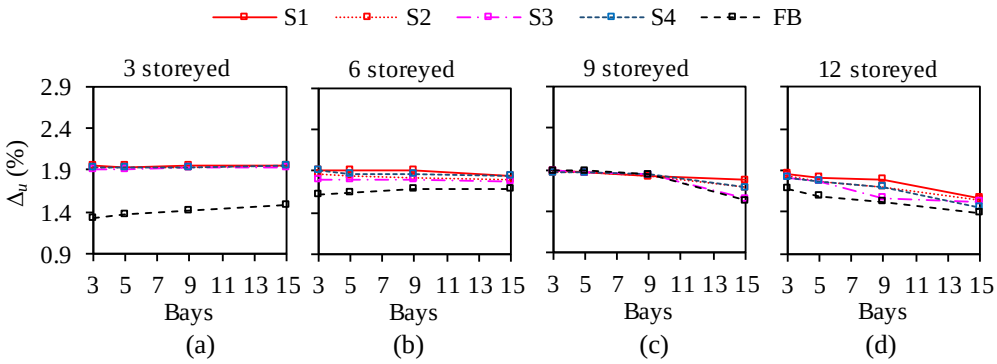

Figure 22. Influence of SPFSI on ultimate drift of RC wall-frame systems of different width and height of (a) 3 storey, (b) 6 storey, (c) 9 storey and (d) 12 storey.

4.3.1. RC Frame System

The ductility capacities of RC frame systems are estimated under the different SPF conditions, and its variation with respect to the FB condition is shown in Figure 23a to 23d. It can be observed that for shorter RC frames (3-storeyed and 6-storeyed), corresponding to almost all the cases, SSI reduces the ductility capacity of the systems due to the attainment of scenario (I). In general, due to the larger magnitude of reduction in Δ_u, the reduction in ductility capacity is observed to be higher for loose soil types (S1 and S2) as compared to the denser soil types (S3 and S4). For instance, corresponding to 6-storeyed frame systems, the largest reduction (12%) in ductility capacity is observed for F6-15 on S1 soil type. Such beahviour can be linked to the large rocking and inelastic pile rotations which lead to peak ISD developing at bottom storey levels; and a simultaneous attainment of lower ISD values at higher storey levels leading to a greater reduction in Δ_u for loose soil types.

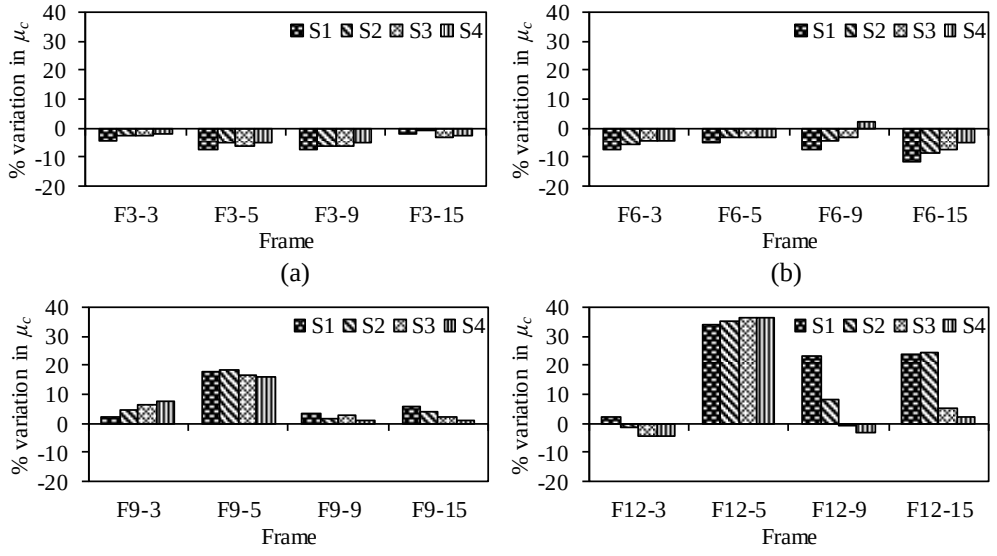

(c) (d)

Figure 23. Variation in ductility capacity under SPFSI for RC frame systems with (a) 3 storeys, (b) 6 storeys,(c) 9 storeys and (d) 12 storeys.

For taller RC frames (9-storeyed and 12-storeyed), barring a few exceptions, SPFSI increases the ductility capacity of the systems due to the attainment of scenario (II). The largest increase in the ductility capacity is observed for F9-5 (19%) and F12-5 (37%) as corresponding to these frames, the increase in the ultimate drift under the SSI cases is observed to be the highest (see Figures 21c and 21d). It should be noted that the increase in ultimate drift is highest for the loose soil (S1 and S2) due to the greater rocking and energy dissipation (in the form of inelastic rotation) exhibited by the pile foundation system, see Figures 16a and 17a), however, the increase in the ductility capacity is not always the highest. Rather, for some frames, the increase in ductility capacity is higher for dense soil types (S3 and S4), for e.g., F9-3 and F12-5. This is because, for these frames, the ultimate drift exhibited in different soil types is of similar order, however, the yield drift in denser soil is relatively lesser, thereby exhibiting a larger increase in the ductility capacity. Corresponding to some of the 12-storeyed frames (F12-3 under S2, S3 and S4 soil; F12-9 under S4 soil), a decrease in ductility capacity is observed due to the attainment of scenario III.

4.3.2 RC Wall-frame System

The variations in the ductility capacity of the considered RC wall-frame configurations with respect to the FB condition are shown in Figures 24a to 24d. For all the 3-storeyed and 6-storeyed wall-frame systems and most of the 9-storeyed and 12-storeyed systems, ductility capacity reduces under SSI effects due to the attainment of scenario (III). It can be observed for several cases that the magnitude of reduction is observed to increase upon increasing the stiffness of the soil from that of S1 to S3 soil. However, on further increasing the stiffness corresponding to that of S4 soil, the reduction in the ductility capacity is observed to be slightly lesser. This is because the increase in the stiffness of the soil from that of S3 to that of S4 causes a slightly greater increase in ultimate drift, thereby exhibiting a relatively lesser reduction in ductility capacity.

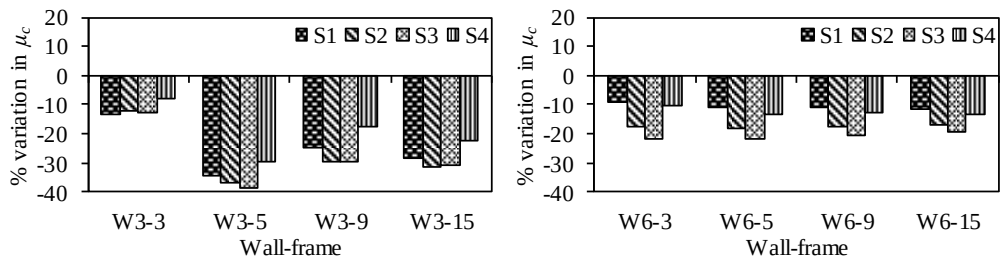

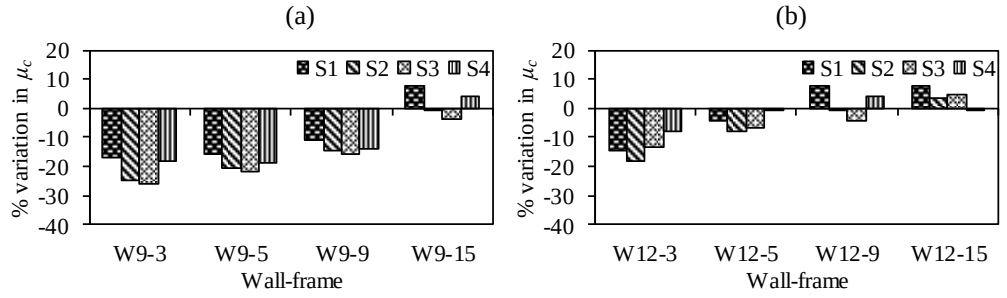

Figure 24. Variation in ductility capacities under the influence of SSI for RC wall-frame systems with (a) 3 storeys, (b) 6 storeys, (c) 9 storeys and (d) 12 storeys.

The largest reduction in ductility capacity for 3-storeyed system was 39% (W3-5 supported by S3 soil); for 6-storeyed system was about 22% (W6-3 supported by S3 soil); for 9-storeyed systems was about 26% (W9-3 supported by S3 soil); and for 12-storeyed system was about 18% (W12-3 supported by S2 soil). For a few wider configurations corresponding to 9-storeyed and 12-storeyed wall-frame systems, an increase in the ductility capacity was observed (e.g., W9-15 supported by S1 and S4 soil; W12-9 supported by S1 and S4 soil; W12-15 supported by S1, S2, and S3 soil) due to the attainment of scenario II. The maximum increase in the ductility capacity was observed for W12-9 supported by S1 soil type and was about 8%. It is worth noting that in several cases, RC wall-frame systems supported on relatively stiffer soil conditions (S3) exhibit greatest reduction in ductility as a result of Δ_u being lower. This is due to the low magnitude of rocking (Figure 16b) resulting from the combined effect of piles (of group 'W') extending to relatively larger lengths in a relatively stiffer soil condition. Also, for the same configurations, the wall-frame systems resting on S4 soil exhibited lesser reduction in ductility capacity, so much so that in some cases it is equal or even lesser than that for S1 soil. This is due to the cross-section as well as the length of plies in group 'W' being the smallest for S4 soil leading to large magnitudes of rocking and pile inelastic rotation (and hence higher Δ_u). The design implications of the observations imply that the reduction in the ductility capacity of wall frame systems can be controlled to some extent by proportioning of the pile geometry (length and cross-section). Further, to account for the reduction in the overall ductility capacity of the systems, suitable modifications in the response reduction factors needs to be adopted at the time of design of RC buildings under SPFSI effects.

5. SUMMARY AND CONCLUSION

In the present study, the influence of soil-pile foundation structure interaction (SPFSI) on the inelastic behaviour and its subsequent effect on the ductility capacity of RC buildings is studied. Numerical models corresponding to a broad

range of configurations of RC frame and RC wall-frame systems supported by pile foundations under different soil conditions have been analysed in OpenSees by conducting nonlinear static pushover analysis. The main conclusions from the present study are as follows:

1. The soil-pile foundation (SPF) system inevitably contributes in the lateral load behaviour of RC buildings and, thus, modifies the inter-storey drift (ISD) profiles (or in other words the inelastic response) of the super structure under the influence of soil pile foundation structure interaction (SPFSI). The exhibited modification eventually governs the increase or decrease in the yield and ultimate drifts exhibited and the extent of this modification is governed by the superstructure and soil-pile-foundation (SPF) characteristics. In general, the effect of SPFSI on the modification of the inelastic behaviour, yield drift and ultimate drifts is considerably greater for RC wall-frame system (compared to RC frame systems) which is further pronounced when supported over loose soil conditions.
2. The modification in the inelastic response of the superstructure due to the presence of soil-pile foundation (SPF) system determines the magnitude of rocking in the pile foundation group. Larger inelasticity within the superstructure reduces the magnitude of rocking in the pile foundation group, and vice versa.
3. The magnitude of plastic rotation in the piles can be correlated with the magnitude of rocking experienced by the pile group. In general, the RC frame and RC wall-frame systems on loose soils exhibit larger inelasticity in the pile foundations. Moreover, low magnitude of compressive loads, stiff superstructure element supported by the pile foundation, and smaller pile geometry leads to greater inelasticity in the piles and greater rocking of the pile group.
4. The incorporation of soil-pile foundation (SPF) system leads to a modification in the ductility capacity of the RC frame and RC wall-frame systems. Stiffer configurations (shorter RC frames and most RC wall-frames) tend to exhibit an overall decrease, while the relatively flexible systems (tall RC frames and RC wall-frame systems) tend to exhibit an overall increase in the ductility capacity. In the present study a maximum decrease in ductility capacity was observed to be 12% and 39% for RC frame and RC wall-frame systems respectively. Whereas the maximum increase in the ductility capacity was found to be about 37% and 8% for RC frame and RC wall-frame systems respectively.
5. Design engineers can adopt suitable modifications in the response reduction factors during the design stage to account for the change in the ductility capacity of RC buildings under SPFSI effects. Although the present

study highlights the potential impact of SPFSI on ductility, future research is crucial to develop specific design guidelines and incorporate modifications to response reduction factors that effectively account for SPFSI effects in seismic design of RC buildings on pile foundations.

Overall, this study reflects the importance of considering the complex phenomenon of soil-pile foundation structure interaction (SPFSI) in assessing the inelastic seismic behaviour of RC buildings and the conclusions from the present study dispels the prevalent notion of "Soil-structure interaction is beneficial in the seismic response". It is worth mentioning that this study has been carried out considering the RC frame and RC wall-frame systems that have been designed and conform to the relevant standard codes prescribed by BIS (Bureau of Indian Standards). Further, the study considers soil material model that most accurately represents cohesionless behaviour of soil. Hence, the conclusion drawn from the study may not be fully applicable to those structures which do not conform to the codal provisions or where the soil cannot be idealized as cohesionless. In such cases complete independent analyses may be required. Future research in the domain of SPFSI of RC buildings can be oriented towards the validation of the findings through static and dynamic experimental studies. Further, design provision to account for the reduction in the ductility of RC buildings under soil-pile-foundation structure-interaction (SPFSI) effects should be developed as the current provisions assume fixed base conditions for the response reduction factors.

ACKNOWLEDGMENTS

The support and resources provided by Dept. of Civil Engg., Indian Institute of Technology Guwahati and Ministry of Human Resources and Development (MHRD, Govt. of India), is gratefully acknowledged by the authors.

ANNEXURE A

Table A1. Details of RC frame members.

No. of stories in building frame	Storey level	Column					Beam				
		Size (mm×mm)	Main reinf.		Shear reinf.		Size (mm×mm)	Main reinf.		Shear reinf.	
			ϕ (mm)	no.	ϕ (mm)	s_v (mm)		ϕ (mm)	no.	ϕ (mm)	s_v (mm)
3	Upto 3	300×300	12	4+4	8 8	75 170	200×280	20† 20*	2 2	8	100
6	Upto 3	350×350	16	4+4	8 8	75 170	200×350	20† 12*	3 3	8	100
	3 to 6	350×350	16 12	4 4	8 8	75 170	200×350	20† 12*	3 3	8	100
9	Upto 3	450×450	16	4+4	8 8	75 170	250×400	20† 12*	4 3	8	100
	3 to 6	400×400	16 12	4 4	8 8	75 200	250×400	20† 12	4 3	8	100
	6 to 9	350×350	16 12	4 4	8 8	75 220	250×350	20† 12*	3 3	8	100

12	Upto 3	500×500	20 16	4 4	8 8	75 170	250×450	25 16*	3 2	8	90
	3 to 6	450×450	16	4+4	8 8	75 200	250×450	25† 16*	3 2	8	90
	6 to 9	400×400	16	4+4	8 8	75 220	250×400	20† 12*	4 3	8	100
	9 to 12	400×400	16 12	4 4	8 8	75 250	200×350	20† 12*	3 3	8	100

Note: ϕ is rebar diameter, † indicates tensile reinf., ∗ indicates compressive reinf. and reinf. is the abbreviation for reinforcement

Table A2. Details of RC shear walls.

No. of Stories	Storey level	Shear wall details					Boundary element details				
			Vertical reinf.		Horizontal reinf.			Main reinf.		Shear reinf.	
		t_w (mm)	ϕ (mm)	no.	ϕ (mm)	s_v (mm)	Size (mm×mm)	ϕ (mm)	no.	ϕ (mm)	s_v (mm)
3	Upto 1	200	12	10*	12	280	500×500	25 20	4 4	8	100
	1 to 3	200	12	10	12	280	300×300	12 12	4 4	8	100
6	Upto 1	200	12	10*	12	280	500×500	25 20	4 4	8	100
	1 to 3	200	12	10	12	280	350×350	16 16	4 4	8	100
	3 to 6	150	12	10	12	300	350×350	16 12	4 4	8	100
9	Upto 1	200	12	10*	12	260	500×500	25 20	4 4	8	100
	1 to 3	150	12	10	12	260	450×450	16 16	4 4	8	100
	3 to 6	150	12	10	12	300	400×400	16 12	4 4	8	100
	6 to 9	150	12	10	12	300	350×350	16 12	4 4	8	100
12	Upto 1	200	12	10*	12	230	500×500	25 20	4 4	8	100
	1 to 3	150	12	10	12	230	500×500	20 16	4 4	8	100
	3 to 6	150	12	10	12	300	450×450	16 16	4 4	8	100
	6 to 9	150	12	10	12	300	400×400	16 16	4 4	8	100
	9 to 12	150	12	10	12	300	400×400	16 12	4 4	8	100

Note: ϕ is rebar diameter, † indicates tensile reinf., ∗ indicates compressive reinf. and reinf. is the abbreviation for reinforcement

Table A3. Details of pile groups supporting frame members.

No. of Stories	Loose Soil S1		Medium soil S2		Med. dense soil S3		Dense soil S4	
	Pile length (m)	Pile dia. (mm)	Pile length (m)	Pile dia. (mm)	Pile length (m)	Pile dia. (mm)	Pile length (m)	Pile dia. (mm)
3	11.0	300	7.0	300	6.5	250	3.5	250
6	12.5	400	7.5	400	5.5	350	4.5	300
9	15.5	450	10.0	450	6.0	400	5.0	350
12	16.5	500	10.5	500	6.5	450	5.0	400

Table A4. Details of pile groups supporting RC shear walls.

No. of Stories	Loose Sand S1		Medium sand S2		Med. dense sand S3		Dense sand S4	
	Pile length (m)	Pile dia. (mm)	Pile length (m)	Pile dia. (mm)	Pile length (m)	Pile dia. (mm)	Pile length (m)	Pile dia. (mm)
3	11.0	250	7.0	250	7.5	200	3.5	200
6	12.5	350	8.5	350	6.5	300	6.5	250
9	17.0	400	11.5	400	8.0	350	7.0	300
12	16.5	500	13.5	450	9.5	400	7.0	350

REFERENCES

[1] Veletsos AS, Meek, JW (1974) Dynamic behaviour of building‐foundation systems. Earthq Eng Struct Dyn 3(2):121–138.

[2] Wolf J. (1985) Dynamic soil-structure interaction. Prentice Hall, Inc..

[3] Luco J, Trifunac M, Wong H (1988) Isolation of soil‐structure interaction effects by full‐scale forced vibration tests. Earthq Eng Struct Dyn 16(1):1–21.

[4] Mittal V, Samanta M, Kanungo DP (2025) Influence of isolated footing embedment on the seismic performance of building considering the soil-foundation-structure interaction: An experimental approach. J Rock Mech Geotech Eng 17(2):1194-1212.

[5] Mittal V, Samanta M (2025) Experimental study on performance of soil-pile-raft-structural system and estimation of piled-raft coefficient under seismic excitations. Eng Struct 325:119440.

[6] El Hoseny M, Ma J, Dawoud W, Forcellini D (2023) The role of soil structure interaction (SSI) on seismic response of tall buildings with variable embedded depths by experimental and numerical approaches. Soil Dyn Earthq Eng 164:107583.

[7] Fiamingo A, Bosco M, Massimino MR (2023) The role of soil in structure response of a building damaged by the 26 December 2018 earthquake in Italy. J Rock Mech Geotech Eng 15(4): 937-953.

[8] Soltani-Azar S (2023) Evaluation of the seismic response of reinforced concrete buildings based on time-history analysis considering nonlinear soil effects. J Earthq Eng 27(7):1690-1710.

[9] Mishra S, Samanta A (2023) Seismic response of multi-storied building with shear wall considering soil-structure interaction in Patna, India. Struct 56:104877.[10] Mylonakis G, Gazetas G (2002) Seismic soil-structure interaction: beneficial or detrimental? J Earthq Eng 4:277–301.

[11] Hassannejad A, Moghaddam AB (2024). A new approach for assessing the contribution of ground motions frequency content and soil-structure interaction to the seismic response of reinforced concrete moment frames. Struct 70:107859).[12] Stewart JP, Fenves GL, Seed RB (1999) Seismic soil-structure interaction in buildings. I: Analytical methods. J Geotech Geoenvironmental Eng 125(1):26-37.

[13] Farghaly AA, Ahmed HH (2013) Contribution of soil-structure interaction to seismic response of buildings. KSCE Journal of Civil Engineering 17:959–971.

[14] Mittal V, Samanta M, Maurya MC (2025) Effect of Soil Constitutive Models and Slenderness Ratios of Piles on Seismic Performance of Moment-Resisting Frames Supported on Pile Foundation Considering Soil–Pile–Structure Interaction. J Struct Des Constr Pract 30(2):04025004.

[15] Mittal V, Samanta M (2025) Influence of Spacing and Slenderness Ratio of End-Socketed Pile Foundation on Seismic Response of Building Considering Soil–Pile–Structure Interaction: An Experimental Approach. J Struct Eng, 151(2):04024213.[16] Ciampoli M, Pinto PE (1995) Effects of soil-structure interaction on inelastic seismic response of bridge piers. J Struct Eng 121(5):806–814.

[17] Hokmabadi AS, Fatahi B, Samali B (2014) Assessment of soil–pile–structure interaction influencing seismic response of mid-rise buildings sitting on floating pile foundations. Comput Geotech 55:172–186.

[18] Gazetas G, Mylonakis G (1998) Seismic soil-structure interaction: New evidence and emerging issues. Geotech Spec Publ 1(75 II):1119–1174.

[19] Han Y (2002) Seismic response of tall building considering soil-pile-structure interaction. Earthq Eng Eng Vibrat 1:57–64.

[20] Fatahi B, Tabatabaiefar SH (2014) Fully nonlinear versus equivalent linear computation method for seismic analysis of midrise buildings on soft soils. Int J Geomech 14(4):04014016.

[21] Nguyen QV, Fatahi B, Hokmabadi AS (2016) The effects of foundation size on the seismic performance of buildings considering the soil-foundation-structure interaction. Struct Eng Mech 58(6):1045–1075.

[22] Carbonari S, Dezi F, Leoni G (2012) Nonlinear seismic behaviour of wall-frame dual systems accounting for soil–structure interaction. Earthq Eng Str Dyn 41:1651–1672.

[23] Paulay T, Priestley MJN (1992) Seismic design of reinforced concrete and masonry buildings. John Wiley and Sons Inc, New York.

[24] BIS (Bureau of Indian Standards) (2016) Indian standard criteria for earthquake resistant design of structures: General provisions and buildings, IS-1893 Part 1, BIS, New Delhi, India.

[25] BIS (Bureau of Indian Standards) (2016) Indian standard ductile detailing of reinforced concrete structures subjected to seismic forces- code of practice, IS-13920, BIS, New Delhi, India.

[26] Arslan MH (2012) Estimation of curvature and displacement ductility in reinforced concrete buildings. KSCE J Civ Eng 16:759–770.

[27] Marzban S, Banazadeh M, Azarbakht A (2014) Seismic performance of reinforced concrete shear wall frames considering soil–foundation–structure interaction. Struct Des Tall Spec Build 23: 302–18.

[28] Mondal A, Ghosh S, Reddy GR (2013) Performance-based evaluation of the response reduction factor for ductile RC frames. Eng Struct 56:1808–1819.

[29] Alhaddad MS, Wazira KM, Al-Salloum YA, Abbas H (2015) Ductility damage indices based on seismic performance of RC frames. Soil Dyn Earthq Eng 77:226–37.

[30] Zerbin M, Aprile A, Beyer K, Spacone E (2019) Ductility reduction factor formulations for seismic design of RC wall and frame structures. Eng Struct 178:102–115.

[31] Ganjavi B, Hao H (2012) A parametric study on the evaluation of ductility demand distribution in multi-degree-of-freedom systems considering soil–structure interaction effects. Eng Struct 43:88–104.

[32] Sharma N, Dasgupta K, Dey A (2018) A state-of-the-art review on seismic SSI studies on building structures. Innov Infrastruct Solut 3:1-16.

[33] Mazzoni S, McKenna F, Scott MH, Fenves GL (2009) Open system for earthquake engineering simulation. User manual, University of California, Berkeley, USA.

[34] ASCE 7-05 (2006) Minimum design loads for buildings and other structures (ASCE Standard ASCE/SEI 7–05). American Society of Civil Engineers, Virginia, USA.

[35] Eurocode 8 Part 1 (2004) Design of structures for earthquake resistance Part 1: General rules, seismic actions and rules for buildings (EN 1998–1: 2004). European Committee for Normalization (CEN), Brussels, Belgium.

[36] Yang Z, Lu J, Elgamal A (2008) OpenSees soil models and solid- fluid fully coupled elements, user's manual version 1.0, University of California, San Diego, USA.

[37] Prevost JH (1985) A simple plasticity theory for frictional cohesionless soils. Soil Dyn Earthq Eng 4(1): 9–17.

[38] Iwan WD (1967) On a class of models for the yielding behavior of continuous and composite systems. J Appl Mech ASME 34:612–617.

[39] Parra E (1996) Numerical modeling of liquefaction and lateral ground deformation including cyclic mobility and dilation response in soil systems. Ph.D. Dissertation, Dept. of Civil Engineering, Rensselaer Polytechnic Institute, Troy, New York, USA.

[40] Drucker DC, Prager W (1952) Soil mechanics and plastic analysis or limit design. Q Appl Math 10:157–165.

[41] Elgamal A, Yang Z, Parra E, Ragheb A (2003) Modeling of cyclic mobility in saturated cohesionless soils. Int J Plast 19:883–905.

[42] Yang Z (2000) Numerical modeling of earthquake site response including dilation and liquefaction. Ph.D. dissertation, Dept. of Civil Engineering and Engineering Mechanics, Columbia University, New York.

[43] Yang Z, Elgamal A, Parra E (2003) Computational model for cyclic mobility and associated shear deformation. J Geotech and Geoenviron Eng 129(12):1119–1127.

[44] Karapetrou ST, Fotopoulou SD, Pitilakis KD (2015) Seismic vulnerability assessment of high-rise non-ductile RC buildings considering soil–structure interaction effects. Soil Dyn and Earthq Eng 73:42-57.

[45] Karafagka S, Fotopoulou S, Pitilakis D (2021) Fragility curves of non-ductile RC frame buildings on saturated soils including liquefaction effects and soil–structure interaction. Bull Earthq Eng 19(15): 6443-6468.

[46] Karafagka S, Fotopoulou S, Pitilakis D (2023) The effect of soil liquefaction and lateral spreading to the seismic vulnerability of RC frame buildings considering SSI. J Earthq Eng 27(16): 4786-4808.

[47] BIS (Bureau of Indian Standards) (1987) Indian standard code of practice for design loads (other than earthquake) for building and structures: Imposed loads. IS-875 Part 2, BIS, New Delhi, India.

[48] BIS (Bureau of Indian Standards) (2000) Indian standard plain and reinforced concrete- code of practice. IS-456, BIS, New Delhi, India.

[49] BIS (Bureau of Indian Standards) (2016) Indian standard ductile detailing of reinforced concrete structures subjected to seismic forces- code of practice. IS-13920, BIS, New Delhi, India.

[50] BIS (Bureau of Indian Standards) (2010) Indian standard design and construction of pile foundations- code of practice: concrete piles, IS-2911 Part 1/Sec 1, BIS, New Delhi, India.

[51] El-Tawil S, Harries KA, Fortney PJ, Shahrooz BM, Kurama Y (2010) Seismic design of hybrid coupled wall systems: state of the art. J Struct Eng 136:755–69.

[52] Menegotto M, Pinto PE (1973) Method of analysis for cyclically loaded reinforced concrete plane frames including changes in geometry and non-elastic behavior of elements under combined normal force and bending moment. In: IASBE Proceedings, pp. 15–22, Lisbon, Portugal.

[53] Filippou FC, Popov EP, Bertero VV (1983) Effects of Bond Deterioration on Hysteretic Behavior of Reinforced Concrete Joints. Report EERC 83-19, Earthquake Engineering Research Center, University of California, Berkeley.

[54] Kent DC, Park R (1971) Flexural members with confined concrete. J Struct Div 97(ST7):1969–1990.

[55] Scott BD, Park R, Priestley MJN (1982) Stress-strain behavior of concrete confined by overlapping hoops at low and high strain rates. ACI 79:13–27.

[56] Wang W, Wang X (2023) Seismic behaviour of structures under long-duration ground motions: A review. Struct 54:1224-1236.

[57] Kazaz İ (2013) Analytical study on plastic hinge length of structural walls. J Struct Eng 139:1938–1950.

[58] Sharma N, Dasgupta K, Dey A (2020) Optimum lateral extent of soil domain for dynamic SSI analysis of RC framed buildings on pile foundations. Front Struct Civ Eng 14:62–81.

[59] Reddy JN (1993) An introduction to the finite element method, McGraw Hill, New York.

[60] Jeremić B, Kunnath S, Xiong F (2004) Influence of soil–foundation–structure interaction on seismic response of the I-880 viaduct. Engineering Structures, 26(3), 391-402.

[61] Pala M, Caglar N, Elmas M, Cevik A, Saribiyik M (2008) Dynamic soil–structure interaction analysis of buildings by neural networks. Constr Build Mater 22(3):330-342.

[62] Rayhani MH, El Naggar MH (2008) Numerical modeling of seismic response of rigid foundation on soft soil. Int J Geomech 8(6):336-346.

[63] Nateghi-A F, Rezaei-Tabrizi A (2013) Nonlinear dynamic response of tall buildings considering structure-soil-structure effects. Struct Des Tall Spec Build 22(14):1075-1082.

[64] Gazetas G (1991) Foundation vibrations. In Foundation engineering handbook (pp. 553-593). Boston, MA: Springer US.

[65] Zhang Y, Yang Z, Bielak J, Conte JP, Elgamal A (2003) Treatment of seismic input and boundary conditions in nonlinear seismic analysis of a bridge ground system. In: 16th ASCE Engineering Mechanics Conference, American Society of Civil Engineers pp. 16-18, University of Washington, Seattle.

[66] Ko YF, Phung C (2014) Nonlinear static cyclic pushover analysis for flexural failure of reinforced concrete bridge columns with combined damage mechanisms. Acta Mech 225(2):477-492.

[67] Thomsen IV JH, Wallace JW (2004) Displacement-based design of slender reinforced concrete structural walls-experimental verification. J of Struct Eng 130(4):618-630.

[68] Zhang Y, Conte JP, Yang Z, Elgamal A, Bielak J, and Acero G (2008) Two-dimensional nonlinear earthquake response analysis of a bridge-foundation-ground system, Earthq Spectra, 24:343–86.

[69] Kolay C, Prashant A, Jain SK (2013) Nonlinear dynamic analysis and seismic coefficient for abutments and retaining walls. Earthq Spectra 29:427–451.

[70] ATC (Applied Technology Council) (1996) Seismic evaluation and retrofit of concrete buildings. ATC-40 Report No. SSC 96–01, ATC, Redwood City, California, USA.

[71] FEMA (Federal Emergency Management Agency) (2000) Pre-standard and commentary for the seismic rehabilitation of buildings, FEMA-356. American Society of Civil Engineers, USA.